Earth Sciences Division

27 October 2015

Dennis Baldocchi
Environmental Science, Policy and Management
University of California, Berkeley

Dear Dennis,

Thank you very much for hosting the AmeriFlux Tech Team site visit at Mayberry (US-Myb) from 08 September – 02 October 2014 (DOY 251-275). This report summarizes the findings and key recommendations from the comparison between the AmeriFlux portable eddy covariance system #1 (PECS1) and the *in situ* system for eddy covariance, radiation, and meteorological observations.

The AmeriFlux PECS1 sensors were deployed to minimize separation (both horizontal and vertical) from the *in situ* sensors (Appendix 1), to avoid interfering with existing infrastructure, and to prevent shadowing or wake effects. The AmeriFlux PECS1 included two gas analyzers: an open-path CO_2 and H_2O infrared gas analyzer (LI-7500A) and an open-path CH_4 analyzer (LI-7700). The PECS1 closed-path infrared gas analyzer (LI-7200) was not operated to reduce power consumption. Data processing of the AmeriFlux PECS1 data was handled by EddyPro® (Version 5.2.1), an open-source eddy covariance software package developed by LI-COR. We are in the process of updating the details of the AmeriFlux data processing and data screening on the AmeriFlux website (ameriflux.lbl.gov). Please contact the AmeriFlux Tech team if you have specific questions.

Four figures were generated for each variable compared. The top figure is a time series of both systems over the evaluation period. The middle figure is a time series of the differences between systems. The lower left figure is a scatter plot of both systems with a 1-to-1 line and a best fit linear regression with equation and fit parameters. Lastly, the lower right figure is a histogram of the differences between the systems with summary statistics. The enclosed figures only include periods where both datasets are available and quality controlled. Missing data periods occurred when data was screened from one or both systems either through data quality checks, outlier removal, environmental interference (precipitation), or no data (power outage) (Figure 1).

Key Recommendations:

Overall, the comparison between the AmeriFlux PECS1 and the *in situ* system was good. We encourage you to continue your active participation in the AmeriFlux network. A few key findings are highlighted below.

- There is a systematic bias with the *in situ* Gill anemometer that impacts the vertical wind component. A small portion is attributed to a digital filter used in the LI-COR 7550 analog inputs. However, the majority is attributed to a bug in the firmware of the *in situ* Gill anemometer (not all Gill anemometers have this issue). We are currently working with and gathering more information from the manufacturers. The manufacturers (Gill and LI-COR) are addressing these issues with new firmware and developing methods for addressing past datasets.
- The CO_2 power spectra of the *in situ* IRGA tailed off above 1 Hz. Please look into this behavior over longer time periods as it could indicate problems with the gas analyzer.
- Methane comparisons were limited due to a faulty gas analyzer on the AmeriFlux PECS (manufacturing error). That said side-by-side comparisons are a valuable means to detect subtle sensor errors.
- The *in situ* net radiometer (over vegetation) was on average 15% smaller than measurements from the PECS1 sensor. Please consider calibrating this instrument.
- We selected 4 comparisons (PAR, sensible heat, latent heat, and CO_2 flux) to benchmark against the network using the accumulated record of site visits since 2002 (see Schmidt et al., 2012). Figure 2 is a histogram of relative instrumental error for each of these terms and how this site visit ranks. For these 4 comparisons, the absolute relative instrumental errors were between 10-22%.

In closing, thank you for your cooperation before, during, and after the site visit. We are actively soliciting comments or feedback regarding the site visit process and report to maximize the utility of our visits. For all reports, we request a summary from the site to describe how the enclosed recommendations will be addressed. I am available to provide further analysis or discussion of the results, if required. Thank you for working collaboratively with the AmeriFlux Tech team.

Please review the general site information table in Appendix 1 of this document and let us know if you notice erroneous information.

All the best,

Stephen Chan[1], Sébastien Biraud[1], David Billesbach[2], Chad Hanson[3]
AmeriFlux Tech team

[1]Lawrence Berkeley National Laboratory
[2]University of Nebraska, Lincoln
[3]Oregon State University

Detailed Report

Data availability:

The PECS1 was deployed from 08 September – 02 October 2014 (Figure 1). This site visit was extended to collect additional observations from the AmeriFlux CH_4 sensor. The PECS1 clock was synchronized to the *in situ* datalogger at the start of the deployment. The PECS1 radiation sensors were removed on 25 September to support another deployment (Figure 1). Data availability from each system is illustrated in Figure 1.

Data processing:

We requested high frequency data to conduct additional comparisons and diagnosis observed differences. We independently processed the high frequency data using EddyPro® software and compared the half-hour results to the provided 'site processing'. Overall, there was excellent agreement between the two datasets. For all metrics compared (means, variances, fluxes), nearly identical results were found (Figure 3 – Figure 6). The variance of CO_2 was the only metric where some scatter around the 1-to-1 line was observed (Figure 7). This difference was attributed to the outlier and despiking routines used. The differences do not appear to affect the CO_2 fluxes (Figure 6). Note that no "angle of attack" corrections were applied to either system despite recent studies which have demonstrated that Gill anemometers may suffer from errors arising from transducer shadowing (Nakai et al., 2006, Nakai and Shimoyama, 2012). Additionally, no spectral/frequency corrections were applied to the *in situ* dataset so the PECS1 results were produced in a similar manner.

Sonic error:

The AmeriFlux Tech Team identified (post site visit) some systematic biases in Gill sonic anemometers. We observed significant underestimations in the variance of the vertical wind (var(w)) compared to the PECS (Figure 25) at some site. The dampened wind components resulted in smaller turbulent fluxes. This problem was only recognized through the cumulative record of datasets collected at recent AmeriFlux site visits (including the Mayberry site visit). Part of the bias was attributed to errors in the LI-COR 7550 analog input channels. The AmeriFlux Tech Team notified LI-COR of this issue in January 2015. At this time, they have confirmed the issue and have firmware versions. However, the majority of the bias appears to be caused by specific ranges (more recent models) of Gill Wind Master and Wind Master

Pros. Gill has acknowledged this problem and are developing a series of communications to address the issue. At this time, it is unclear how the “angle of attack” corrections (Nakai) are related.

For the comparison of turbulent fluxes, a secondary time series was produced from the *in situ* high frequency data. We applied a multiplicative factor to the vertical wind component in an effort to account for the sonic error. For this site visit, we found that a factor of 1.13 applied to the vertical wind brought the sonic variances into close agreement. Please note that this is an empirical ‘correction’ factor. We do not recommend applying this factor as part of your data processing. The manufacturer will be releasing more information soon.

For the enclosed figures, a few different data sources were used for the Mayberry results. “In situ” refers to the results as provided by the site staff. “Mayberry EP“ refers to the AmeriFlux Tech Team processing using Eddy Pro and the *in situ* high frequency data. “Mayberry EP w113“ refers to the AmeriFlux Eddy Pro processing results with a multiplicative factor of 1.13 applied to the vertical wind component.

Turbulent fluxes:

All *in situ* turbulent fluxes were smaller on average compared to the PECS1 due dampened sonic anemometer signal (see “Data acquisition error” section). CO_2 fluxes had the largest disagreement between the *in situ* and the AmeriFlux observations (slope: 0.76, offset: -0.27 μmol m^{-2} s^{-1}, R^2 = 0.93) (Figure 8). The comparison improved when the empirical correction factor was applied but the *in situ* CO_2 fluxes were still smaller by 15 percent (Figure 8). We could not definitely pinpoint the source of the remaining difference but have some suggestions. The *in situ* IRGA’s CO_2 had a slightly smaller CO_2 variance compared to the PECS (Figure 18). Furthermore, the CO_2 power spectra (FIG) tailed-off around 1 Hz indicating that it may not be capturing all high frequency signals.

The *in situ* latent heat fluxes were approximately 10% smaller compared to the PECS1 (slope: 0.89, offset: 0.84 W m^{-2}, R^2 = 0.97) (Figure 9) while the sensible heat fluxes were 15% smaller (slope: 0.85 offset: 2.85 W m^{-2}, R^2 = 0.98) (Figure 10). After the empirical correction factor was applied, both sensible and latent heat fluxes were in very close to a 1:1 relationship with the PECS1 data (Figure 9 and Figure 10). The *in situ* friction velocity was less affected by the data acquisition issue (Figure 11).

The ensemble averaged spectra and cospectra for relevant terms are provided (Figure 12 and Figure 13). Both figures summarize data from the entire comparison period. The PECS1 methane spectrum was very unusual and attributed to a faulty sensor (described below). The power spectra for *in situ* sonic temperature and CO_2 (Figure 12) both tailed-off around 1 Hz. This could result from noisy signal but it is difficult to attribute the source. Please take a closer look at this behavior over longer time periods. The normalized cospectra (Figure 13) between the two systems agreed fairly closely. Although it is difficult to see in the figure, the *in situ* w'co2' cospectra was smaller in magnitude relative to the PECS1 which is consistent with the difference found in the CO2 fluxes (Figure 8).

To place these results in the context of the broader AmeriFlux network, we selected a few metrics (sensible heat, latent heat, CO_2 fluxes) to benchmark (Figure 2) against the accumulated record of AmeriFlux site visits since 2002 (Schmidt et al., 2012). To accomplish this, we changed the reference value from a site maximum (equation 1, Schmidt et al., 2012) to a fixed value (see Figure 1).

Methane:

This site visit was the inaugural deployment of the AmeriFlux fast response methane sensor (LI-COR 7700). The AmeriFlux sensor was identical (make/model) and was configured identically (heater, washer/spin settings) to the in situ sensor. Mean methane concentrations (Figure 14) had reasonable agreement but there were significant differences in the standard deviations (Figure 15), fluxes (Figure 16), and power spectra (Figure 12). The PECS1 methane signal was very noisy. LI-COR determined that the PECS1 sensor was faulty and it was replaced. They have developed new engineering tests to address the problem. This paired comparison proved critical in identifying a manufacturing defect.

IRGA scalars and statistics:

The mean CO_2 mole densities from the *in situ* and the PECS1 open-path IRGAs were in close agreement (slope: 1.02, offset: -0.37 mmol m^{-3}, R^2 = 0.91) (Figure 17). The variance of CO_2 was also in reasonable agreement, but slightly smaller, considering that some of the difference was due to the specific despiking routine used (slope: 0.82, offset: 0.00 (mmol $m^{-3})^2$, R^2 = 0.86) (Figure 18).

The mean H_2O mole densities agreed well but a small offset was present (slope: 1.01, offset: 32.90 mmol m^{-3}, R^2 = 0.96) (Figure 19). The variance of H_2O was very similar between the systems (slope: 1.08, offset:

5.91 (mmol m^{-3})^2, R^2 = 0.98) (Figure 20). Unlike CO_2 variance, there was no difference between the in situ and AmeriFlux EddyPro processed results (Figure 20).

Sonic wind components and temperature:

The mean horizontal wind speed (slope: 1.00, offset: 0.01 m s^{-1}, R^2 = 1.00) (Figure 21) and wind direction from the sonic anemometers was excellent (slope: 0.98, offset: 4.77^o, R^2 = 1.00) (Figure 22).

The rotated wind component variances from the *in situ* dataset all agreed within a few percent for the horizontal components (Figure 23 and Figure 24). As previously discussed, the *in situ* anemometer had smaller variance in the vertical wind component compared to the PECS1 sonic anemometer due to a systematic bias in the *in situ* anemometer and the analog input channels used (slope: 0.78, offset: -0.01 m s^{-1}, R^2 = 0.99) (Figure 25).

Sonic temperature statistics were not provided but were calculated from the high frequency dataset. Sonic temperature means (Figure 26) and variances (Figure 27) were in good agreement between the two systems.

Meteorological and radiation measurements:

Air temperature (Figure 28) and relative humidity (Figure 29) measurements were good agreement although a small offset of 4% in relative humidity was seen. Differences in the barometric pressure were extremely small (Figure 30).

Two sets of upwelling measurements were made at the site: over open water and over vegetation (Appendix 1). The enclosed comparisons use the *in situ* measurements over vegetation since the PECS1 sensors were similarly deployed over vegetation. The *in situ* net radiometer reported 15% smaller values compared to the PECS1 sensor with daytime differences near 100 W m^{-2} (slope: 0.85, offset: -10.42 W m^{-2}, R^2 = 0.99) (Figure 31). Please consider calibrating this sensor. The in incoming situ PAR measurements were 10% larger than the PECS1 (slope: 1.10, offset: 1.48 W m^{-2}, R^2 = 0.99) (Figure 32). Upwelling PAR measurements were very similar on average but some hysteresis suggests that a sensor was out-of-level (slope: 0.99, offset: 0.33 W m^{-2}, R^2 = 0.99) (Figure 33).

References:

Nakai, T., Shimoyama, K., 2012. Ultrasonic anemometer angle of attack errors under turbulent conditions. Agric. For. Meteorol. 162–163, 14–26.

Nakai, T., van der Molen, M.K., Gash, J.H.C., Kodama, Y., 2006. Correction of sonic anemometer angle of attack errors. Agric. For. Meteorol. 136, 19–30.

Schmidt, A., C. Hanson, W. S. Chan, and B. E. Law (2012), Empirical assessment of uncertainties of meteorological parameters and turbulent fluxes in the AmeriFlux network, J. Geophys. Res., 117, G04014, doi:10.1029/2012JG002100.

Table of Figures:

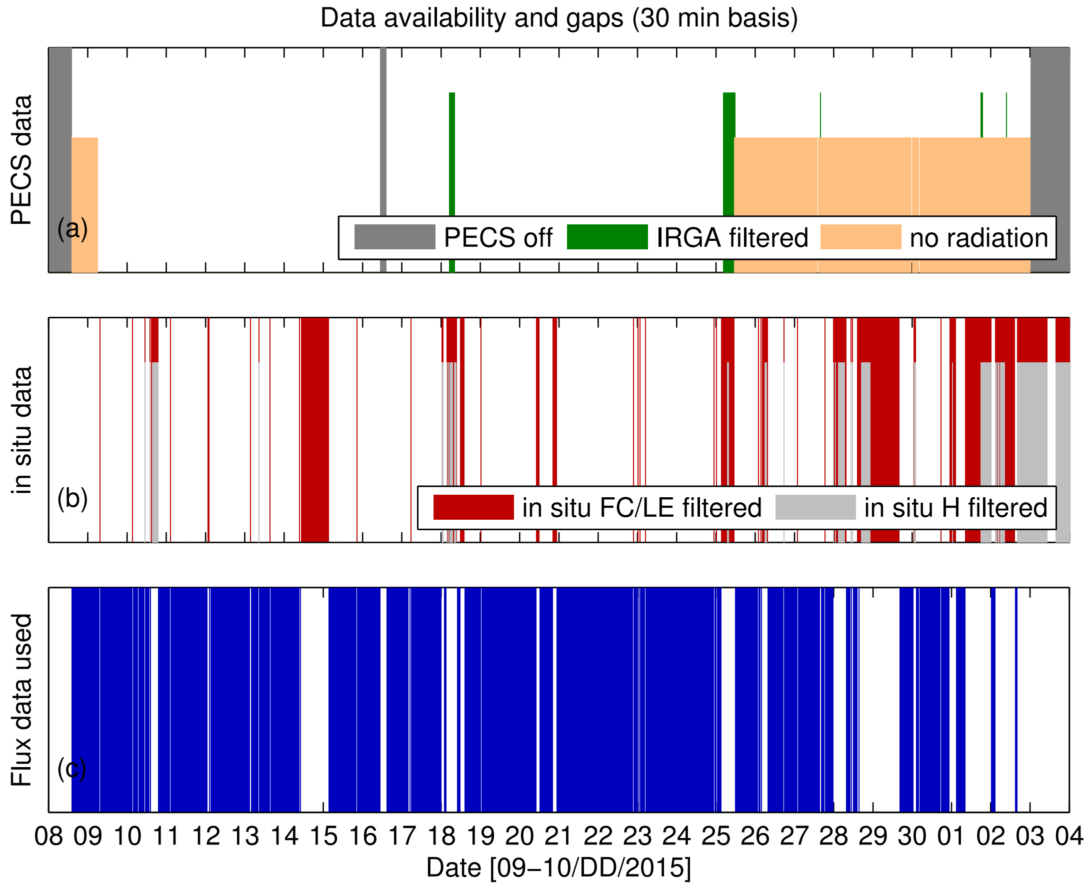

Figure 1 – Data availability for the PECS1 (panel a). PECS1 radiometers were removed early to support another deployment. I*n situ* data filtering (panel b) of sensible heat fluxes (H) and CO_2/H_2O fluxes (FC, LE). The data used for the inter-comparison (panel c).

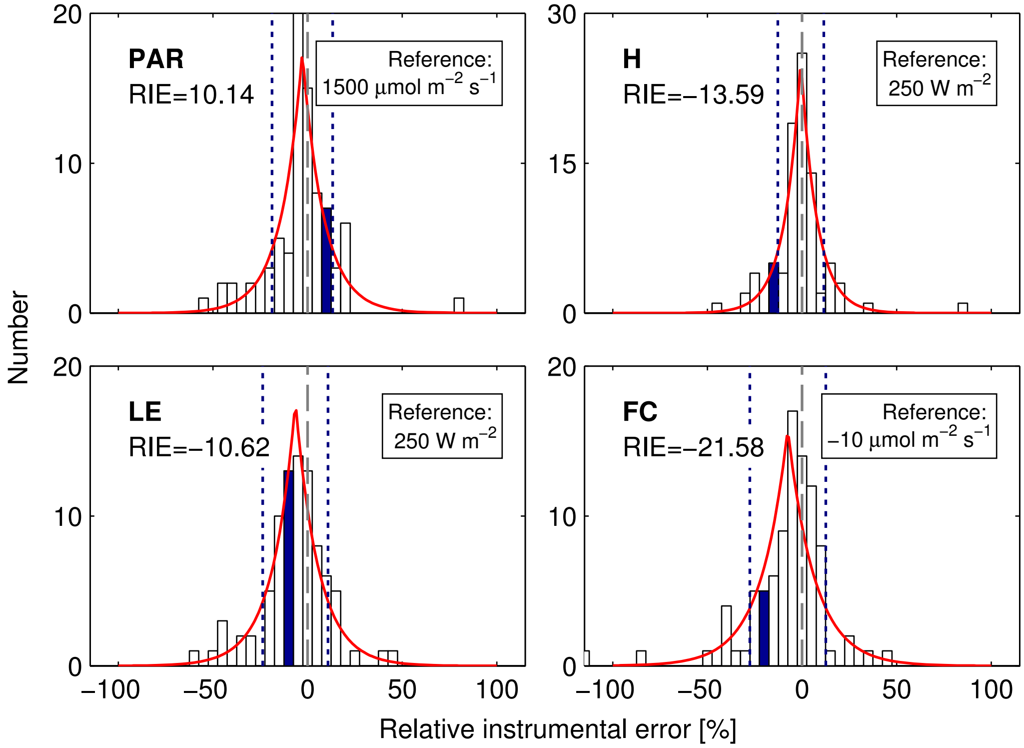

Figure 2 – Histogram of relative instrumental error (RIE) for 4 selected variables based on the accumulated record of AmeriFlux site visits. Colored bar denotes the RIE from this site visit (bar width = 5%). Laplace distribution illustrated in solid red line. Dashed, vertical lines denote mean ± √2β, where β is a scale parameter describing the Laplace distribution. The term √2β is equivalent to the standard deviation in a normal distribution.

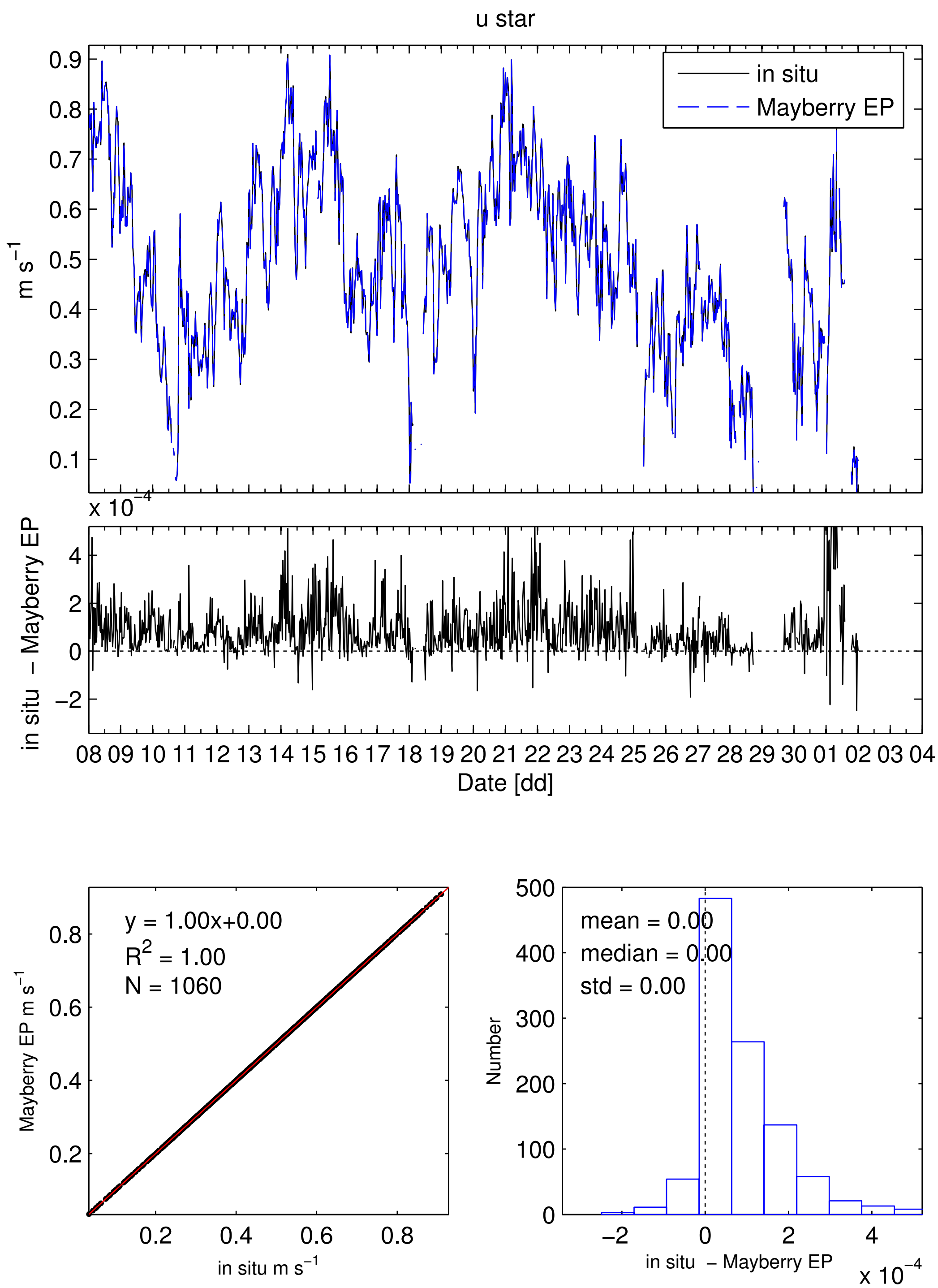

Figure 3 – Friction velocity from site processing (*in situ*) compared to EddyPro© results produced by the AmeriFlux Tech Team (Mayberry EP) using provided high frequency data.

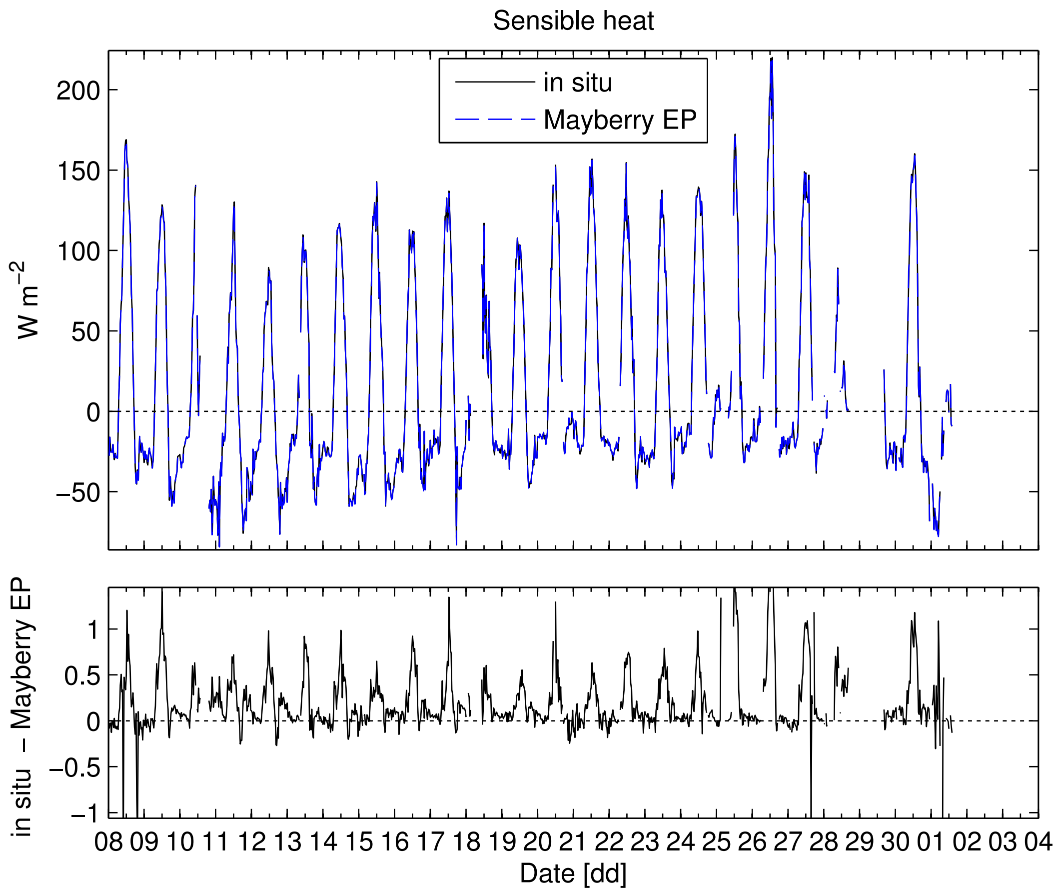

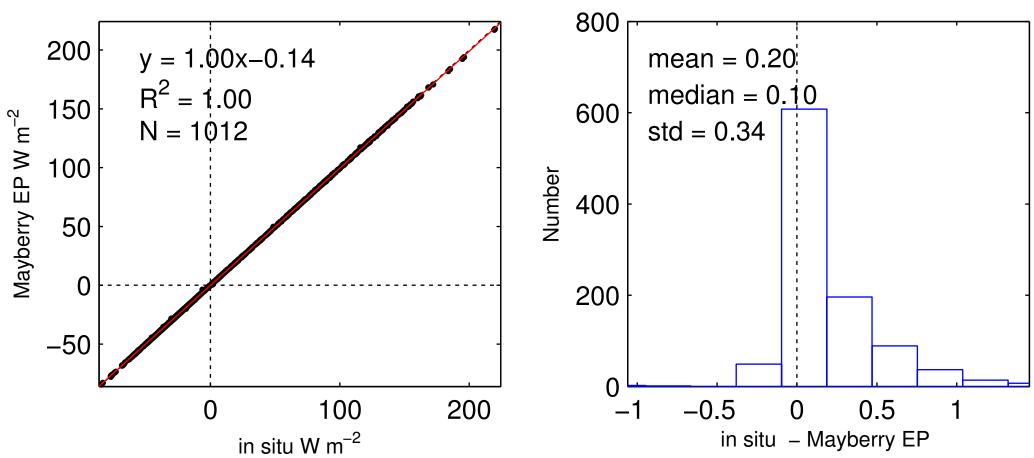

Figure 4 – Sensible heat fluxes from site processing (*in situ*) compared to EddyPro© results produced by the AmeriFlux Tech Team (Mayberry EP) using provided high frequency data.

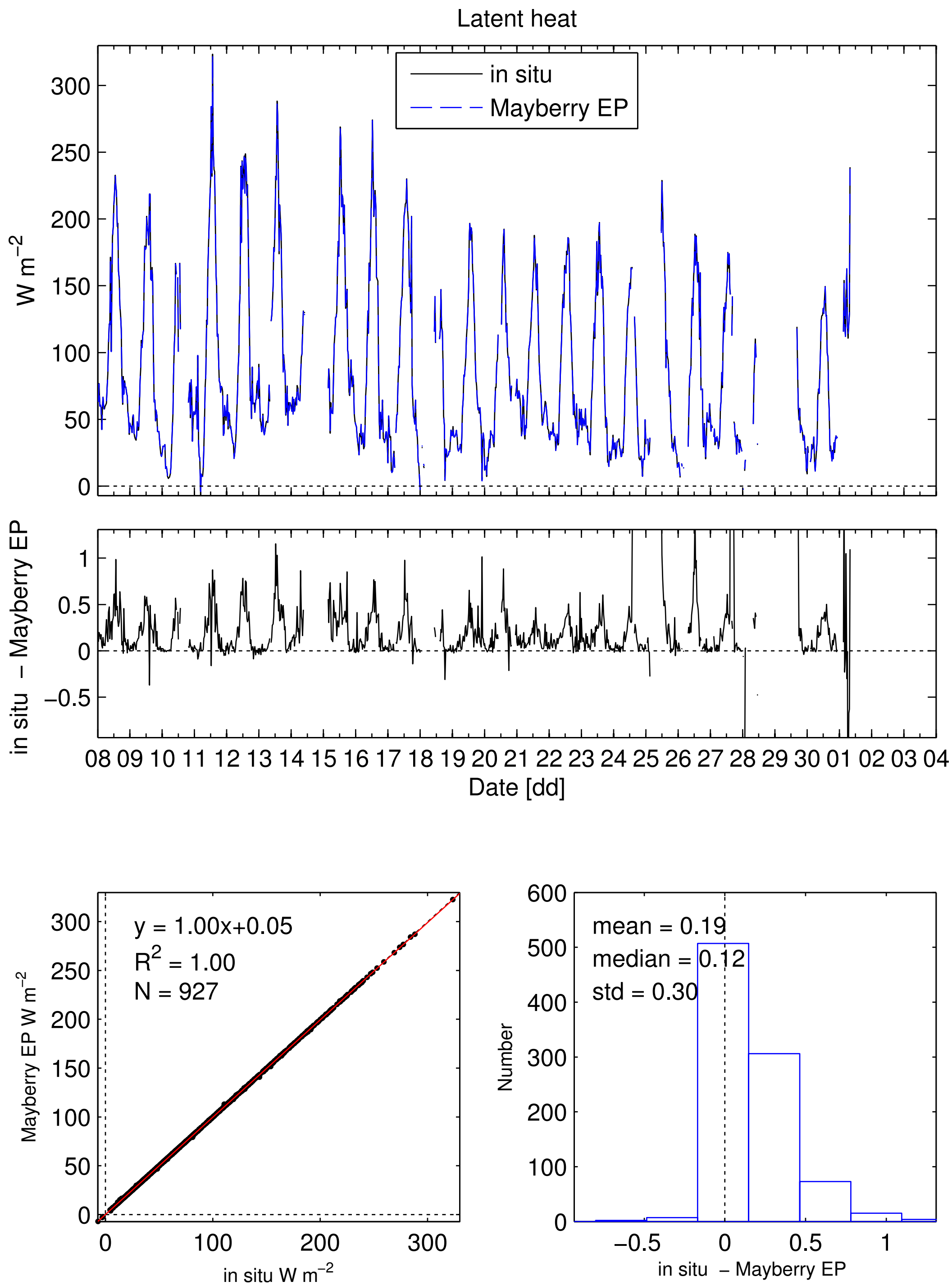

Figure 5 – Latent heat fluxes from site processing (*in situ*) compared to EddyPro© results produced by the AmeriFlux Tech Team (Mayberry EP) using provided high frequency data.

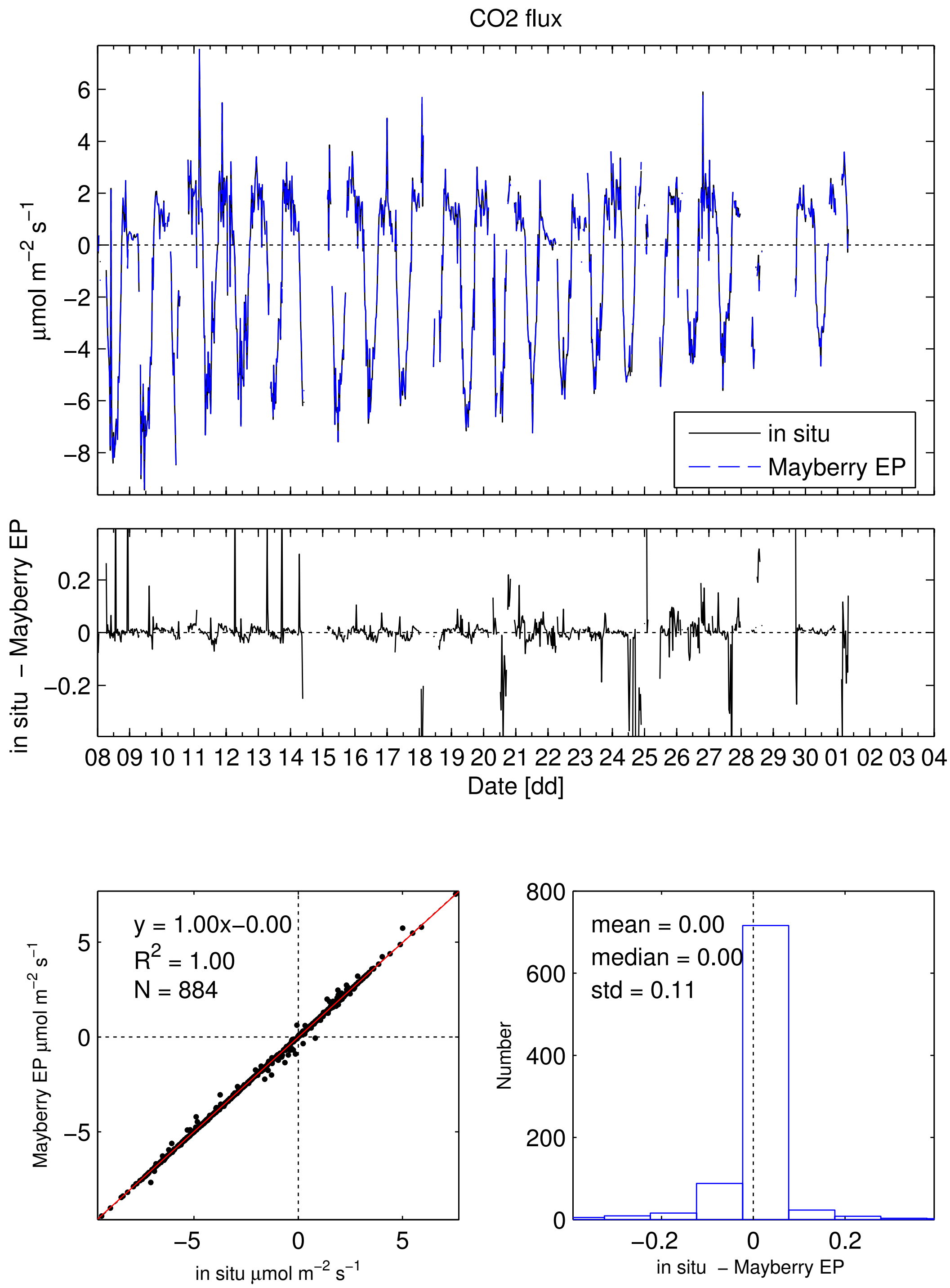

Figure 6 – CO_2 fluxes from site processing (*in situ*) compared to EddyPro© results produced by the AmeriFlux Tech Team (Mayberry EP) using provided high frequency data.

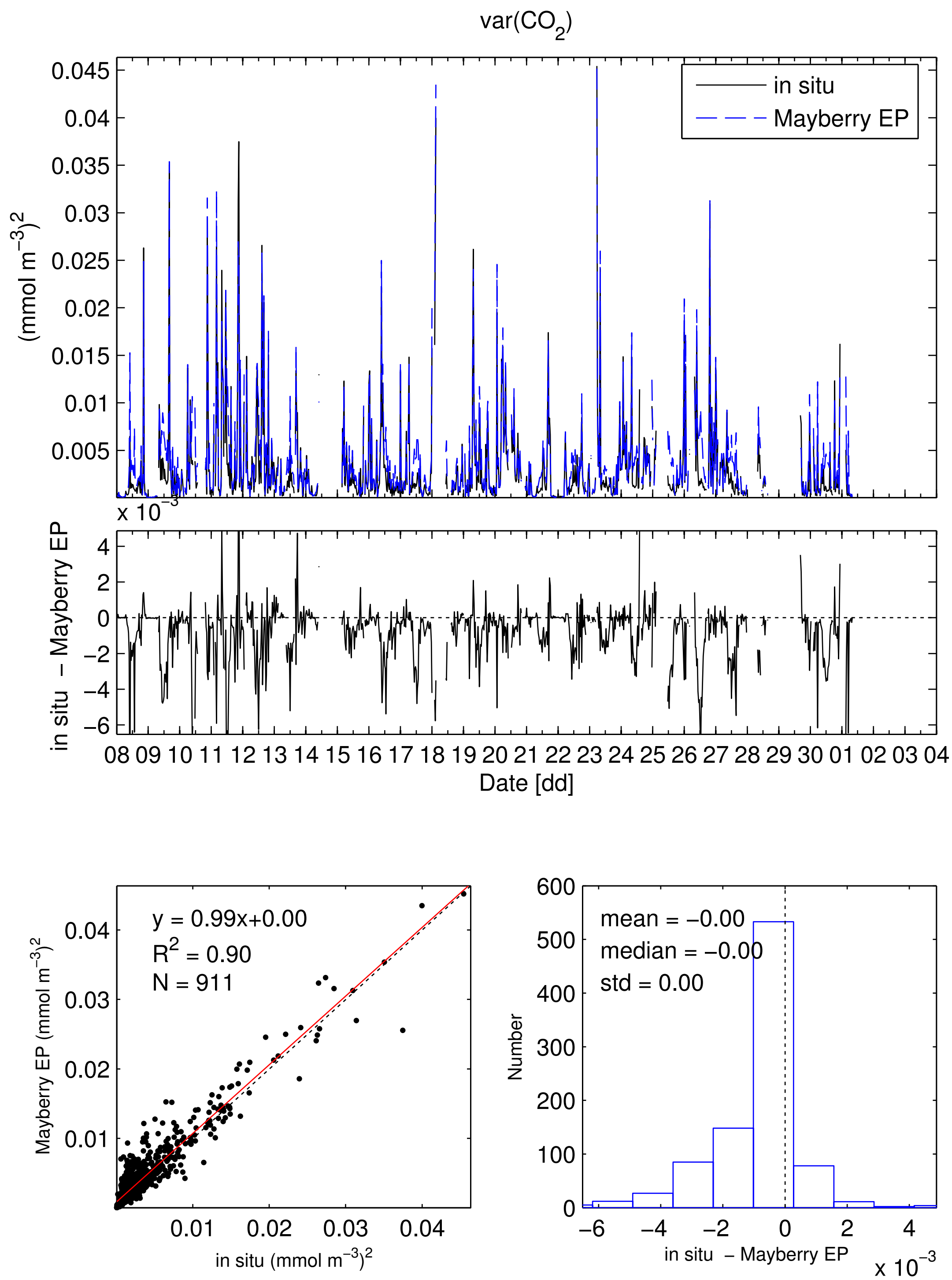

Figure 7 – Variance of CO_2 from site processing (*in situ*) compared to EddyPro© results produced by the AmeriFlux Tech Team (Mayberry EP) using provided high frequency data.

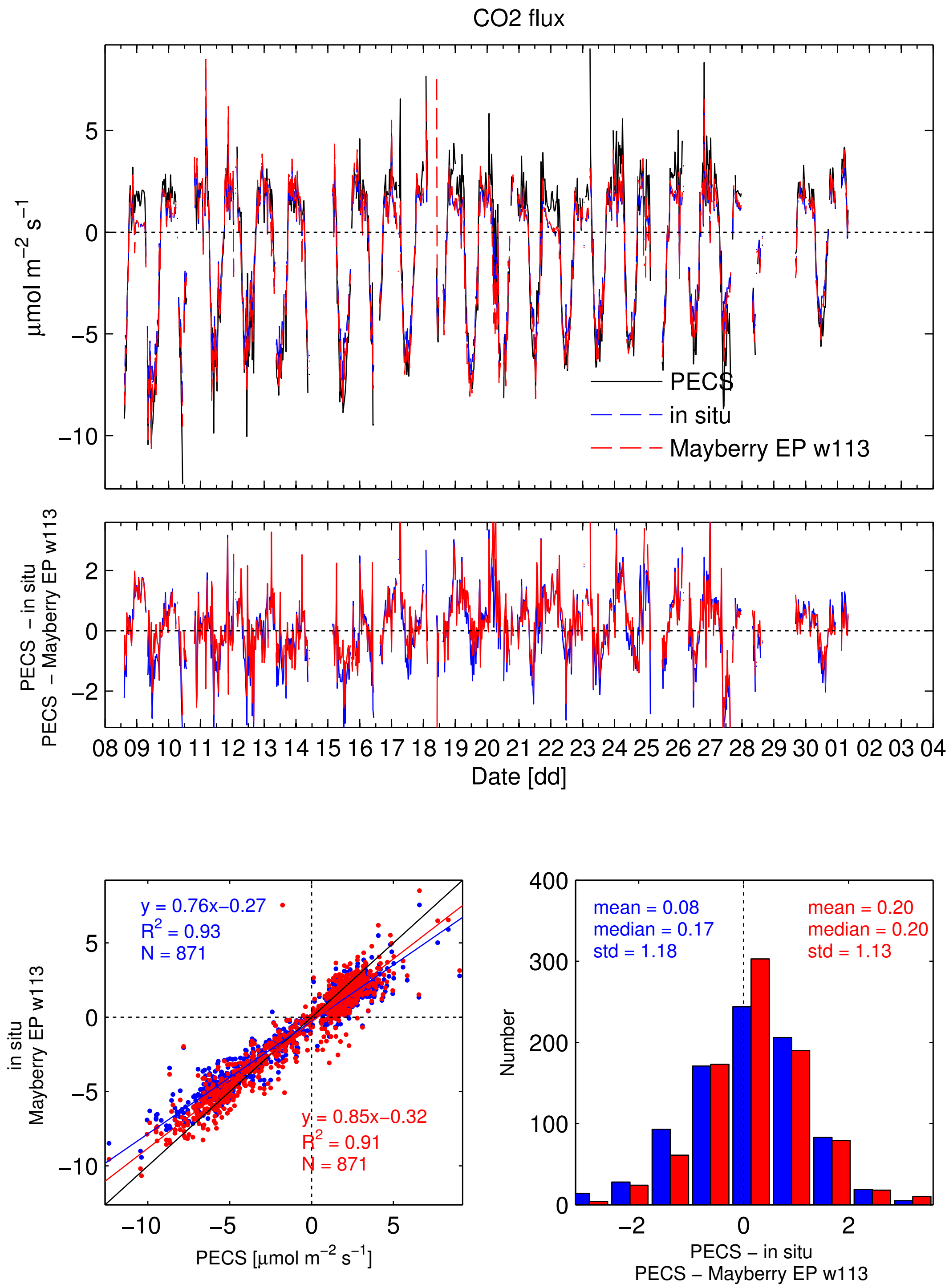

Figure 8 – CO_2 fluxes. “Mayberry EP w113” denotes dataset with factor of 1.13 applied to vertical wind.

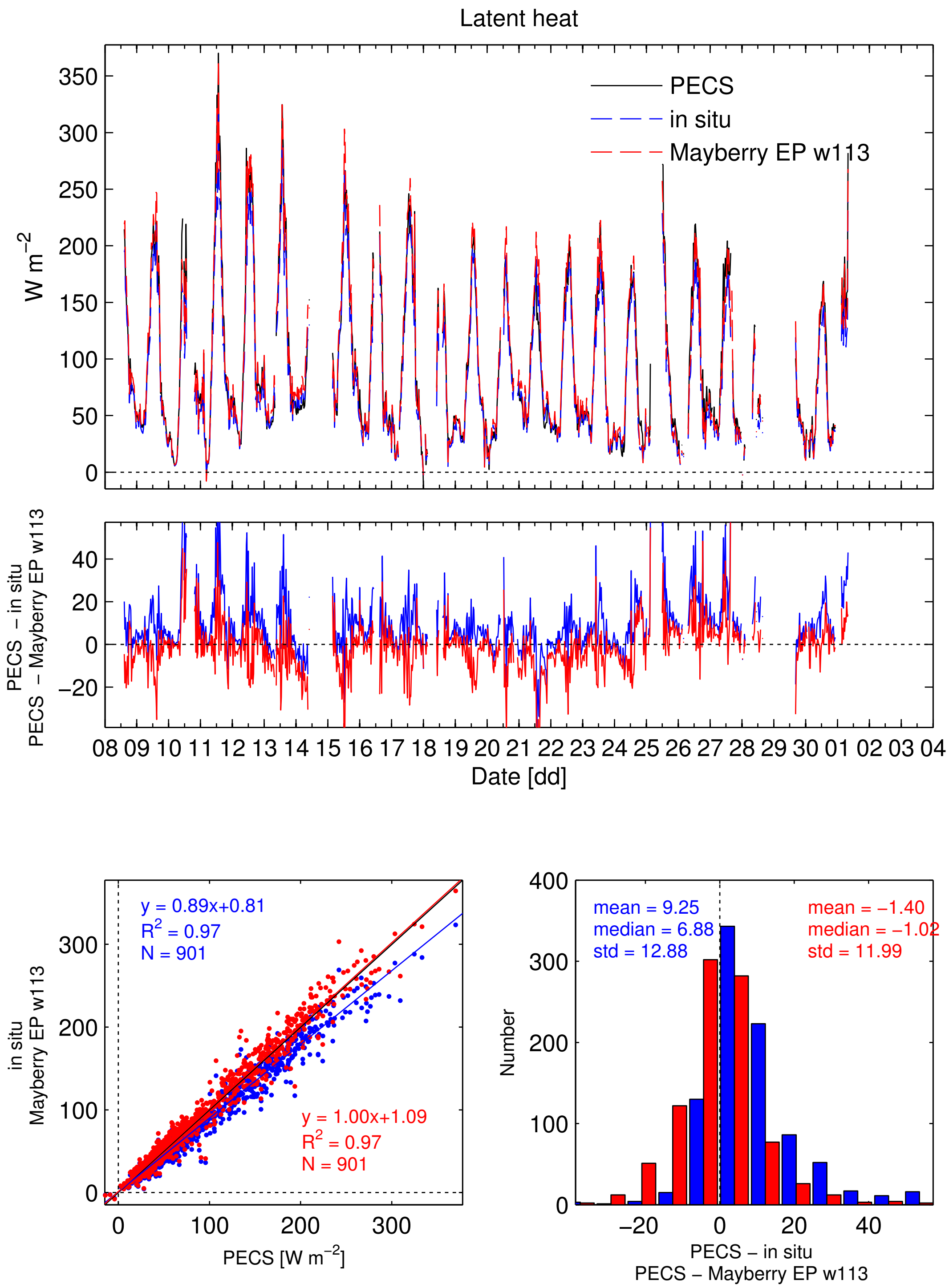

Figure 9 – Latent heat flux. "Mayberry EP w113" denotes dataset with factor of 1.13 applied to vertical wind.

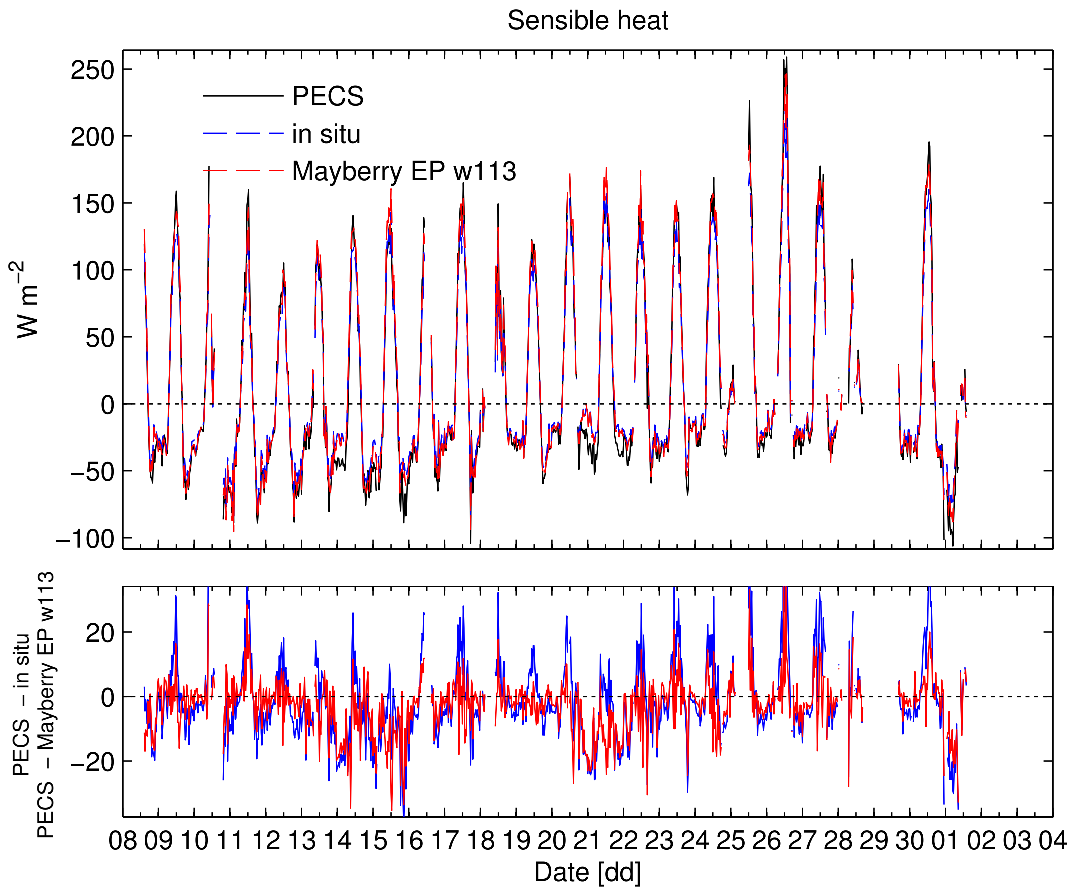

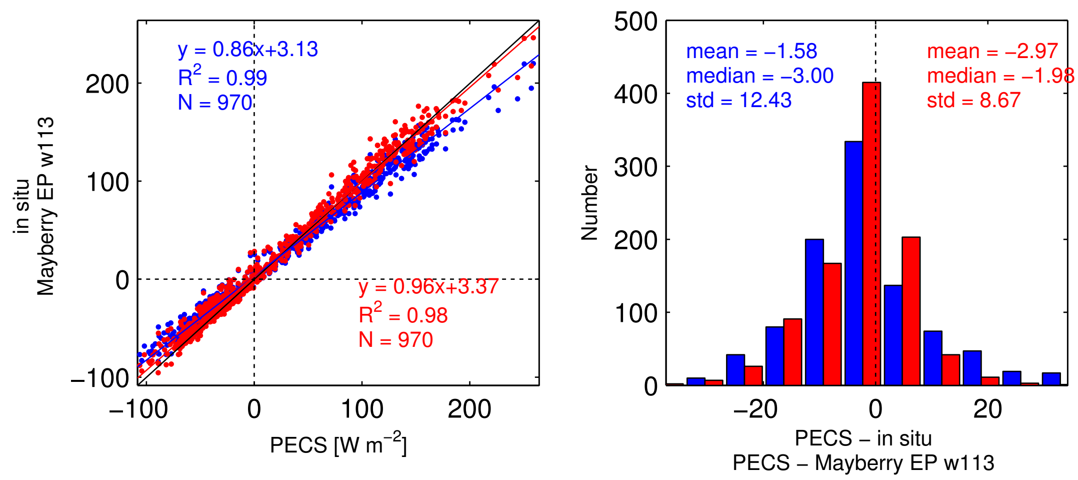

Figure 10 – Sensible heat flux. "Mayberry EP w113" denotes dataset with factor of 1.13 applied to vertical wind.

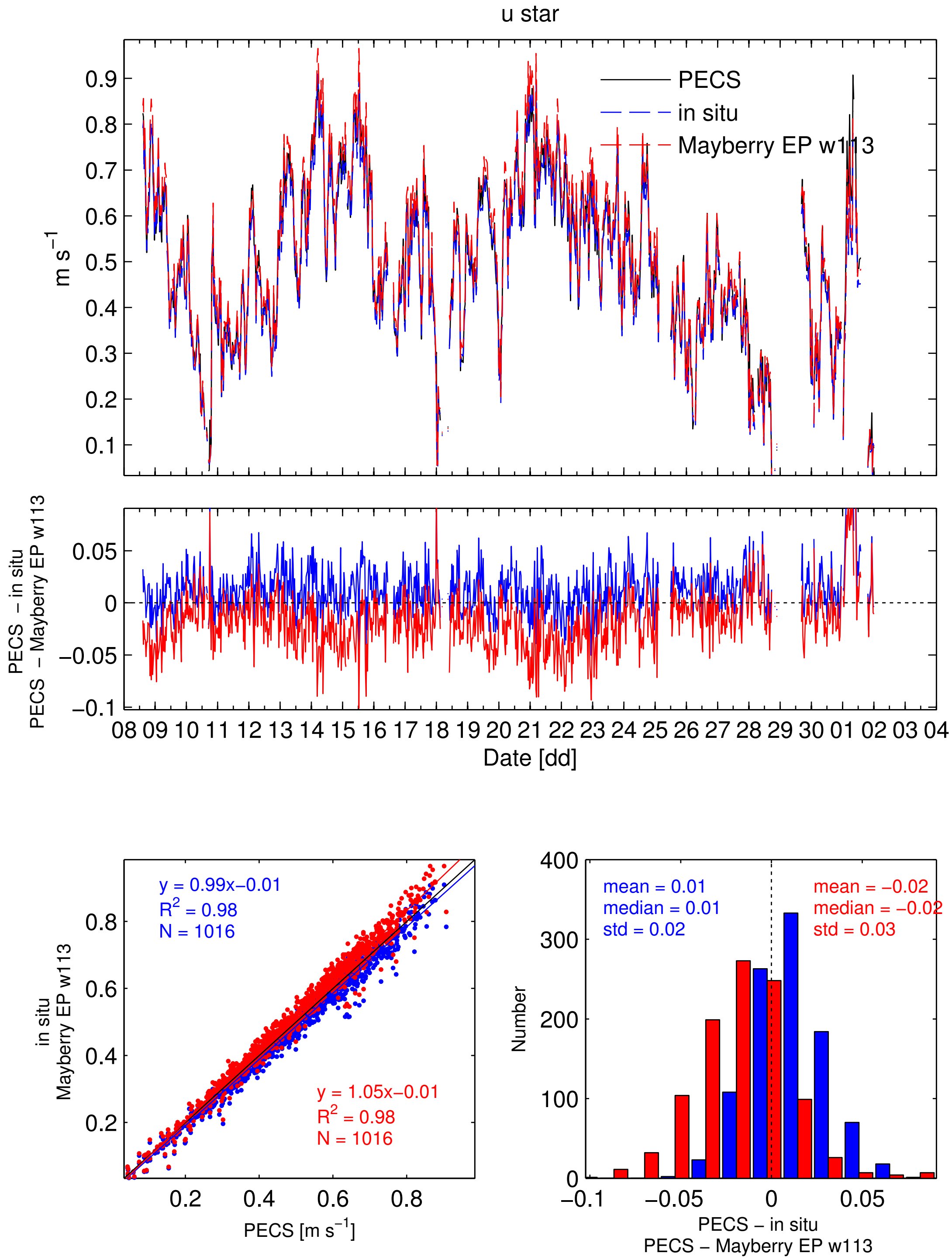

Figure 11 – Friction velocity. “Mayberry EP w113” denotes dataset with factor of 1.13 applied to vertical wind.

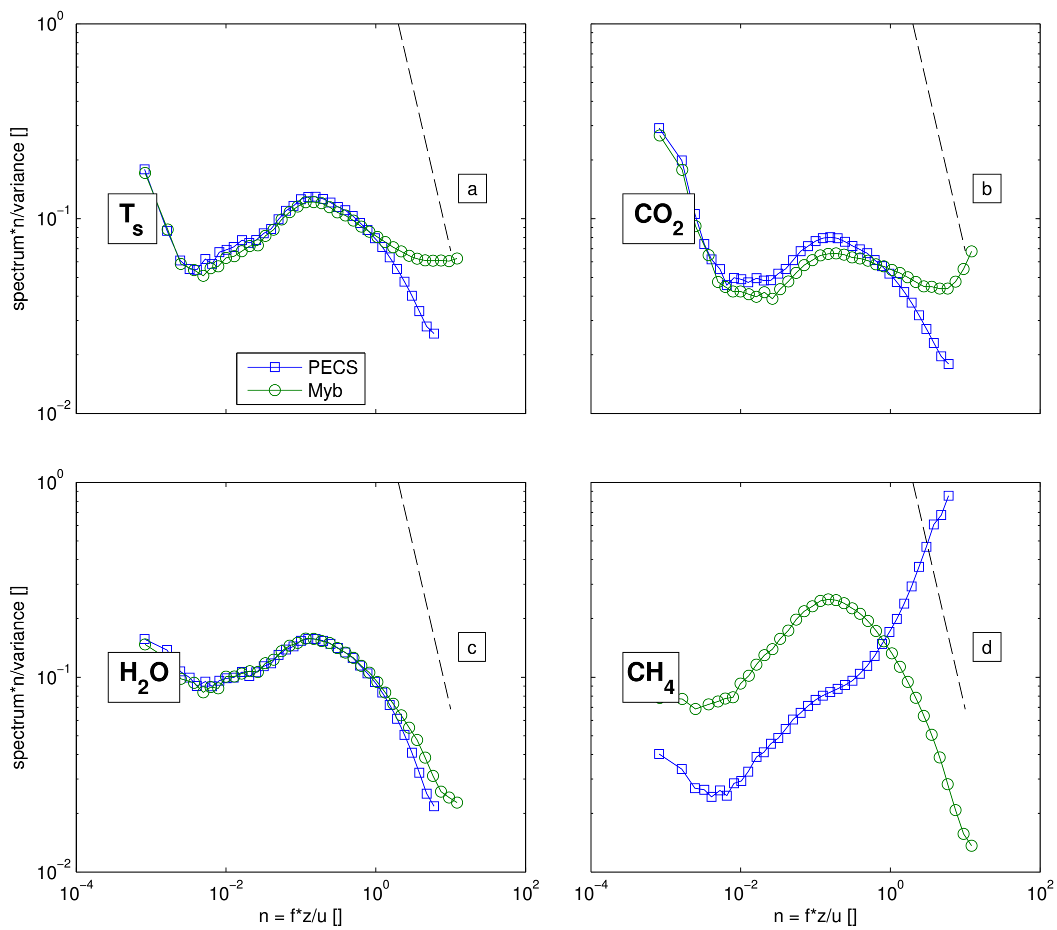

Figure 12 – Ensemble averaged power spectra for sonic temperature (a), CO_2 (b), water vapor (c), and methane (d).

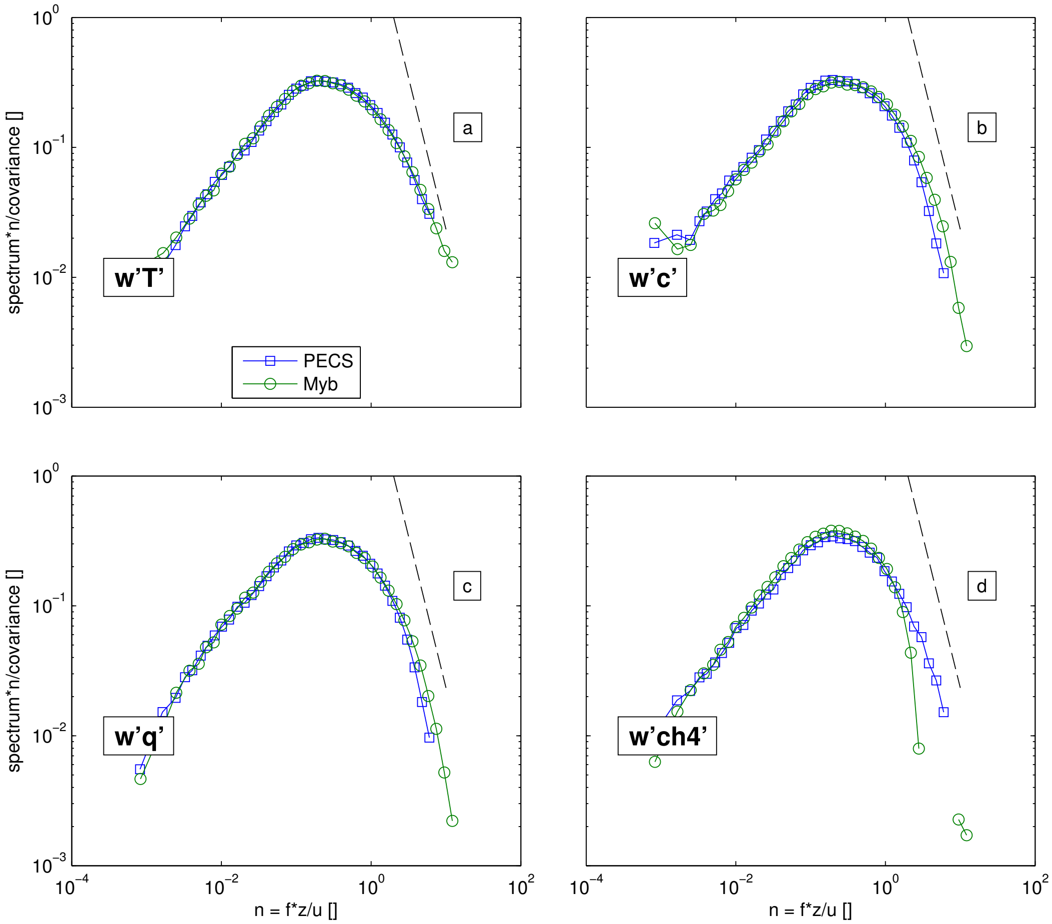

Figure 13 – Ensemble averaged cospectra for terms representing kinematic heat flux (a), carbon dioxide flux (b), latent heat flux (c), and methane flux (d).

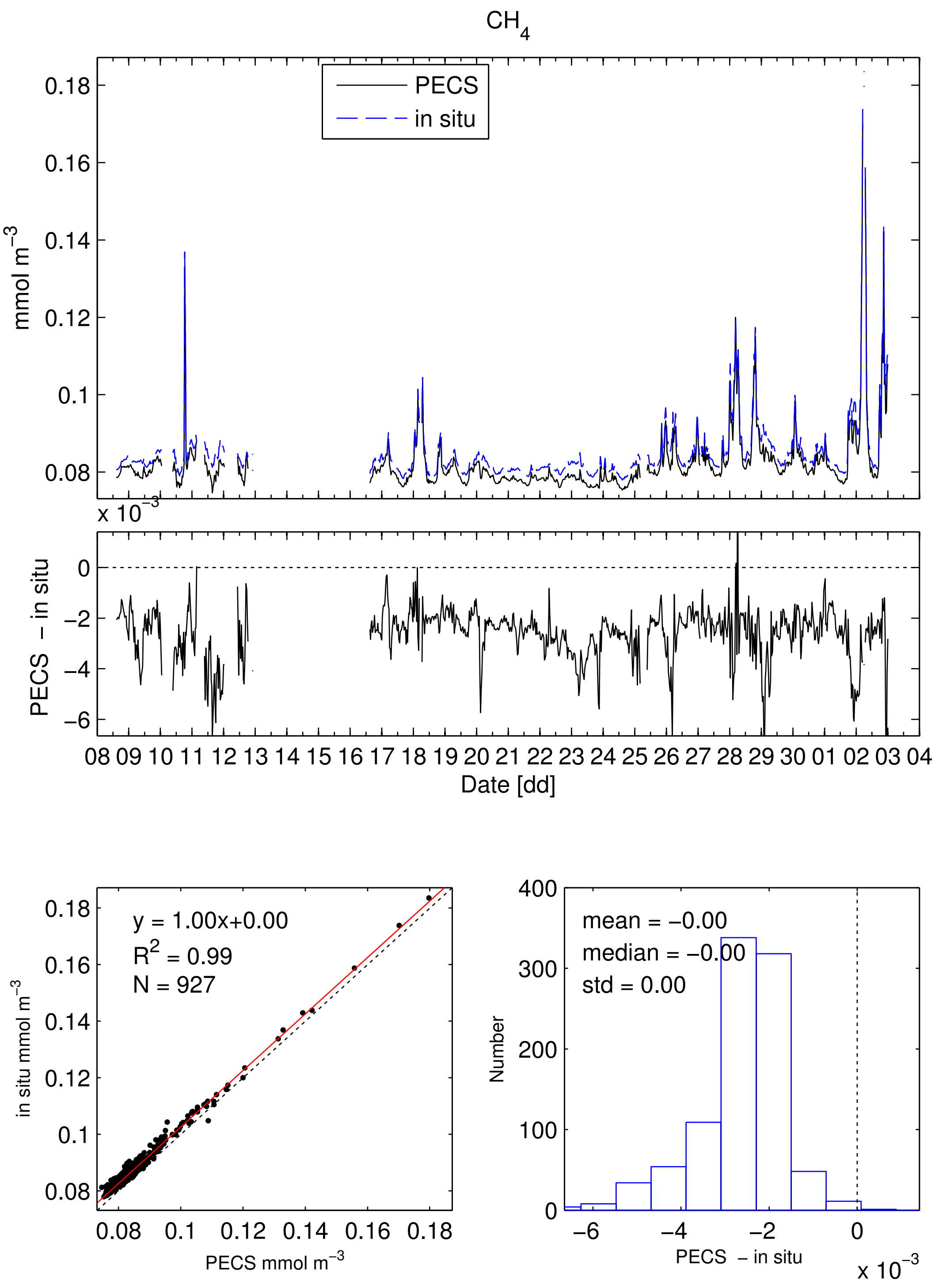

Figure 14 – Methane mole density.

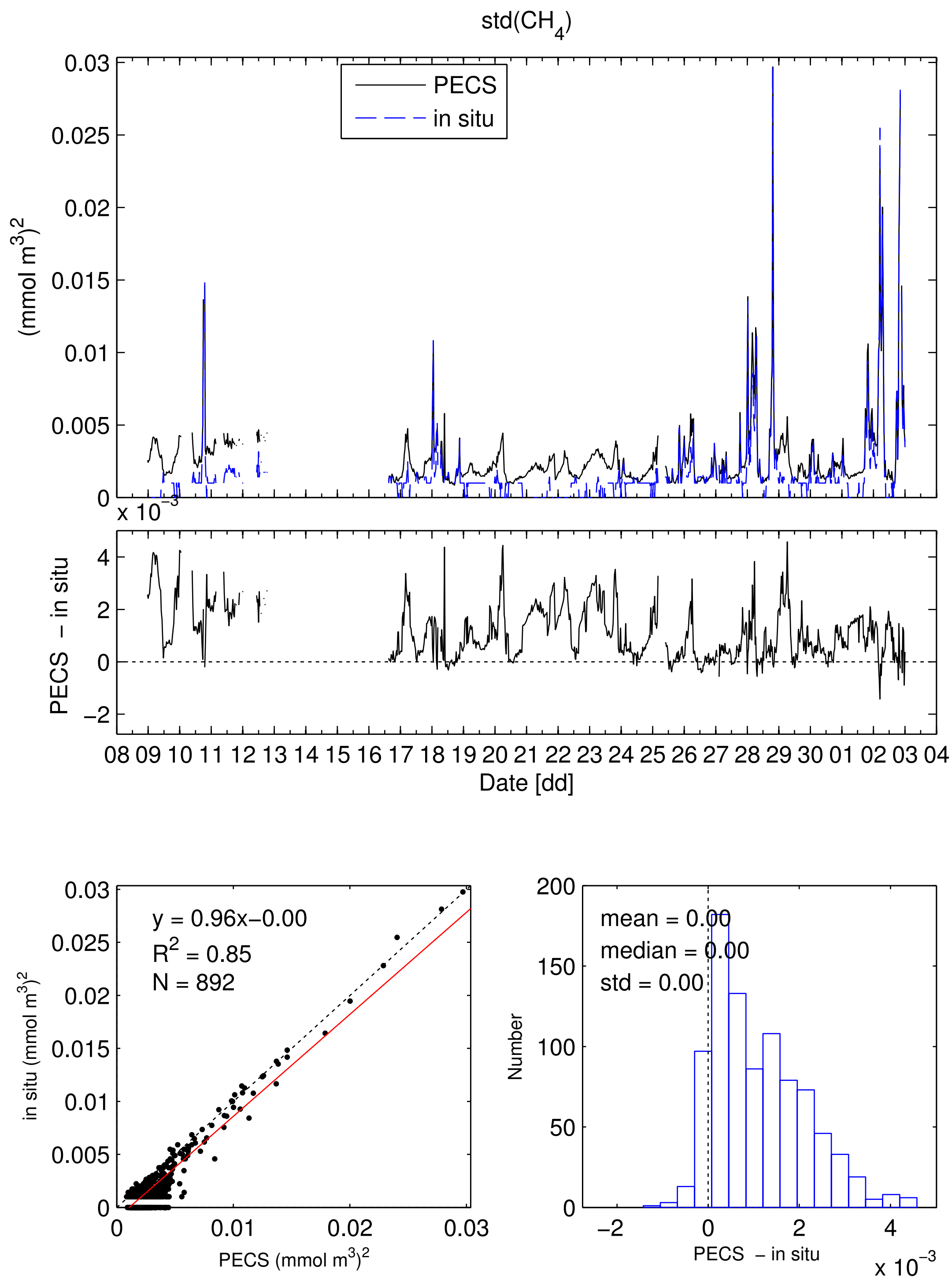

Figure 15 – Standard deviation of methane mole density.

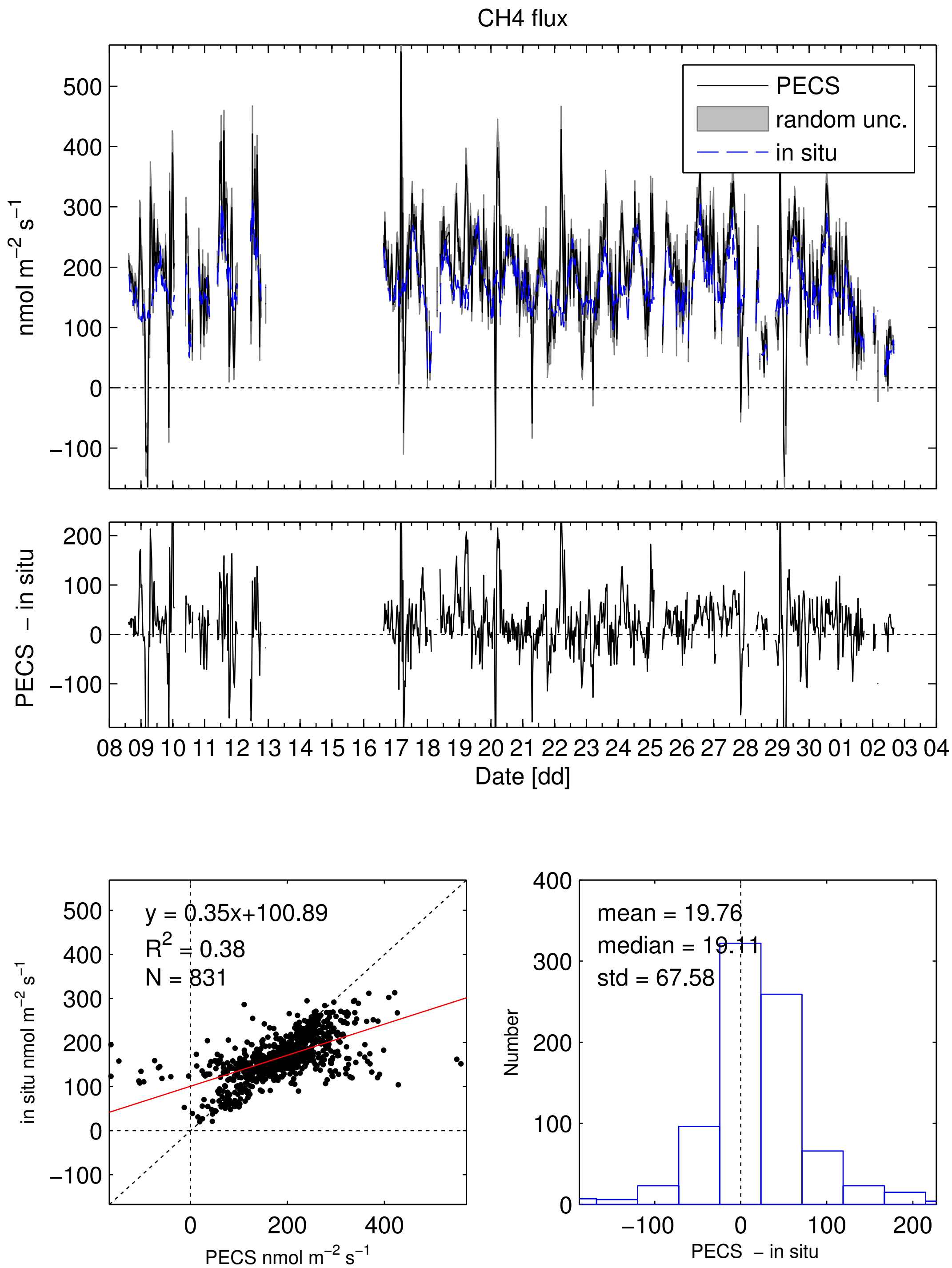

Figure 16 - Methane fluxes.

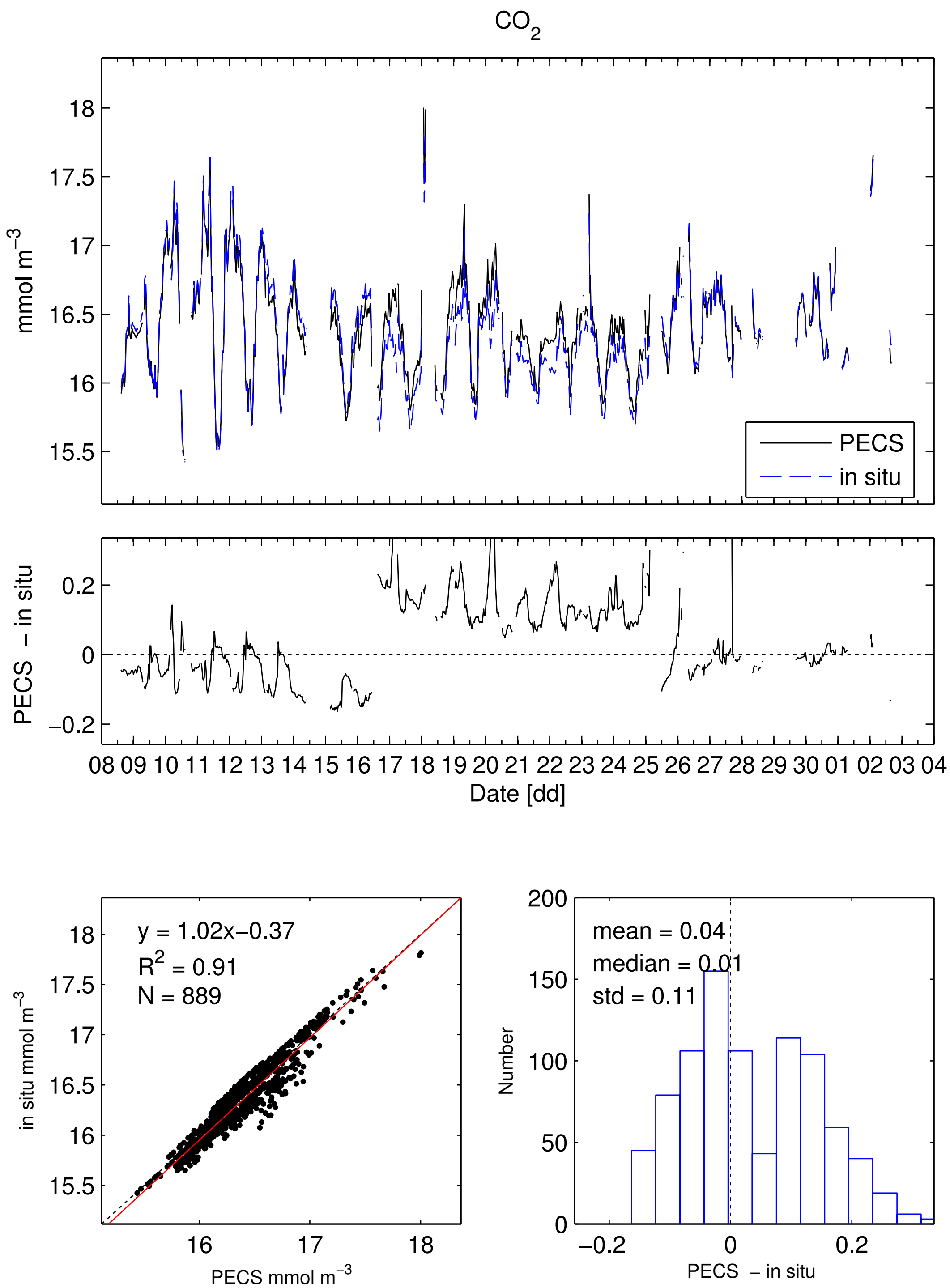

Figure 17 – CO_2 mole density.

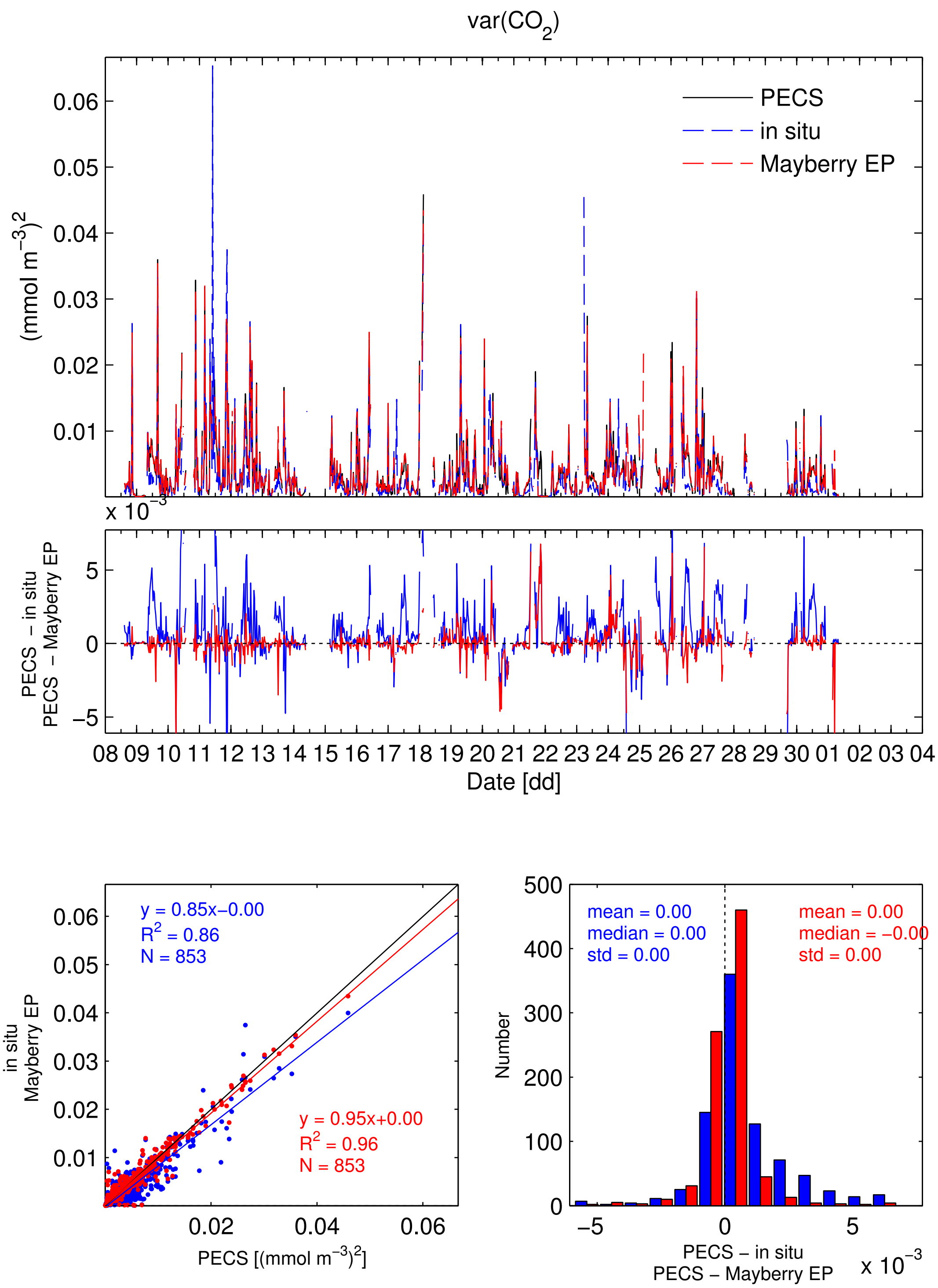

Figure 18 – Variance of carbon dioxide mole density.

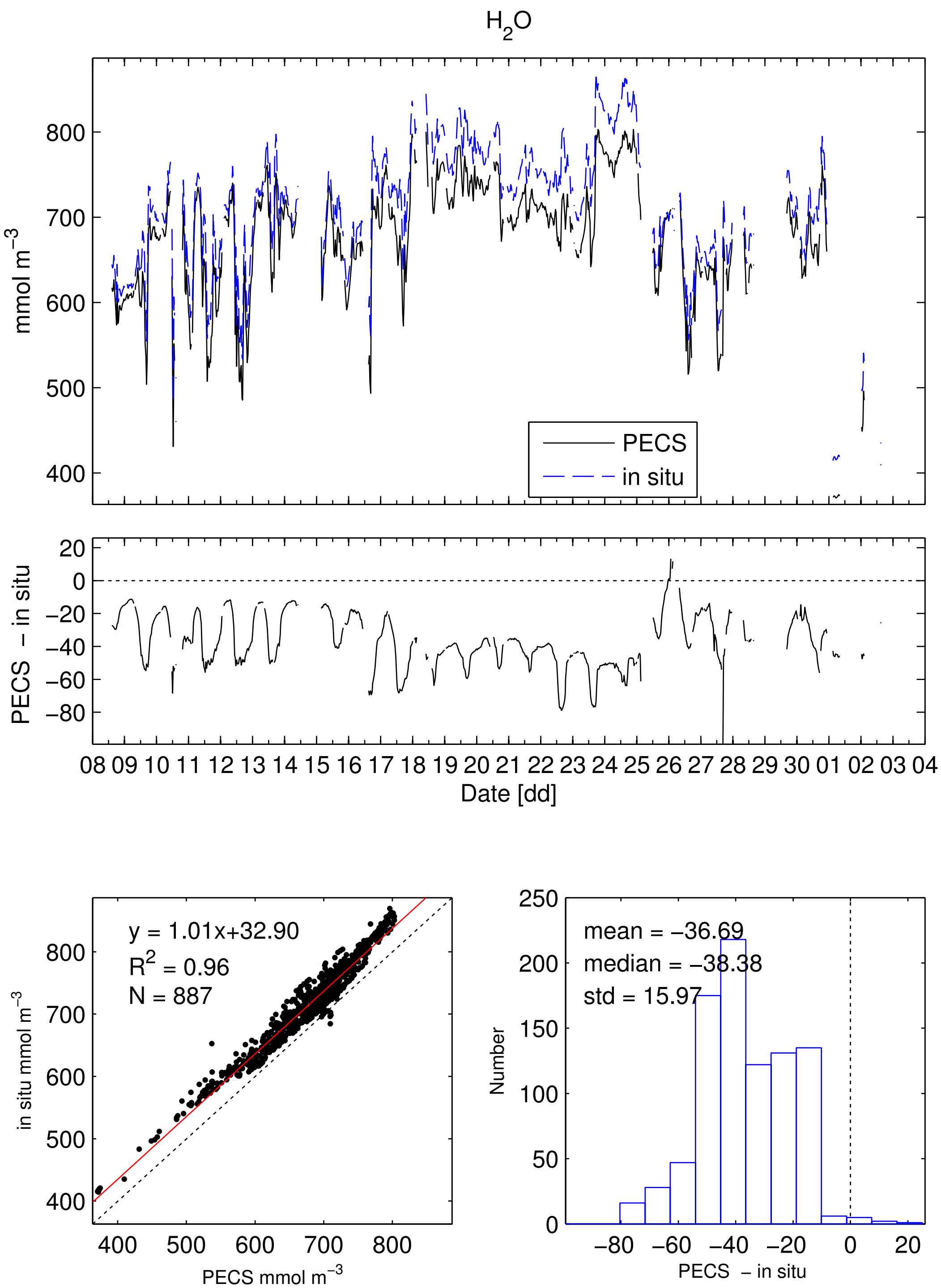

Figure 19 – Water vapor mole density.

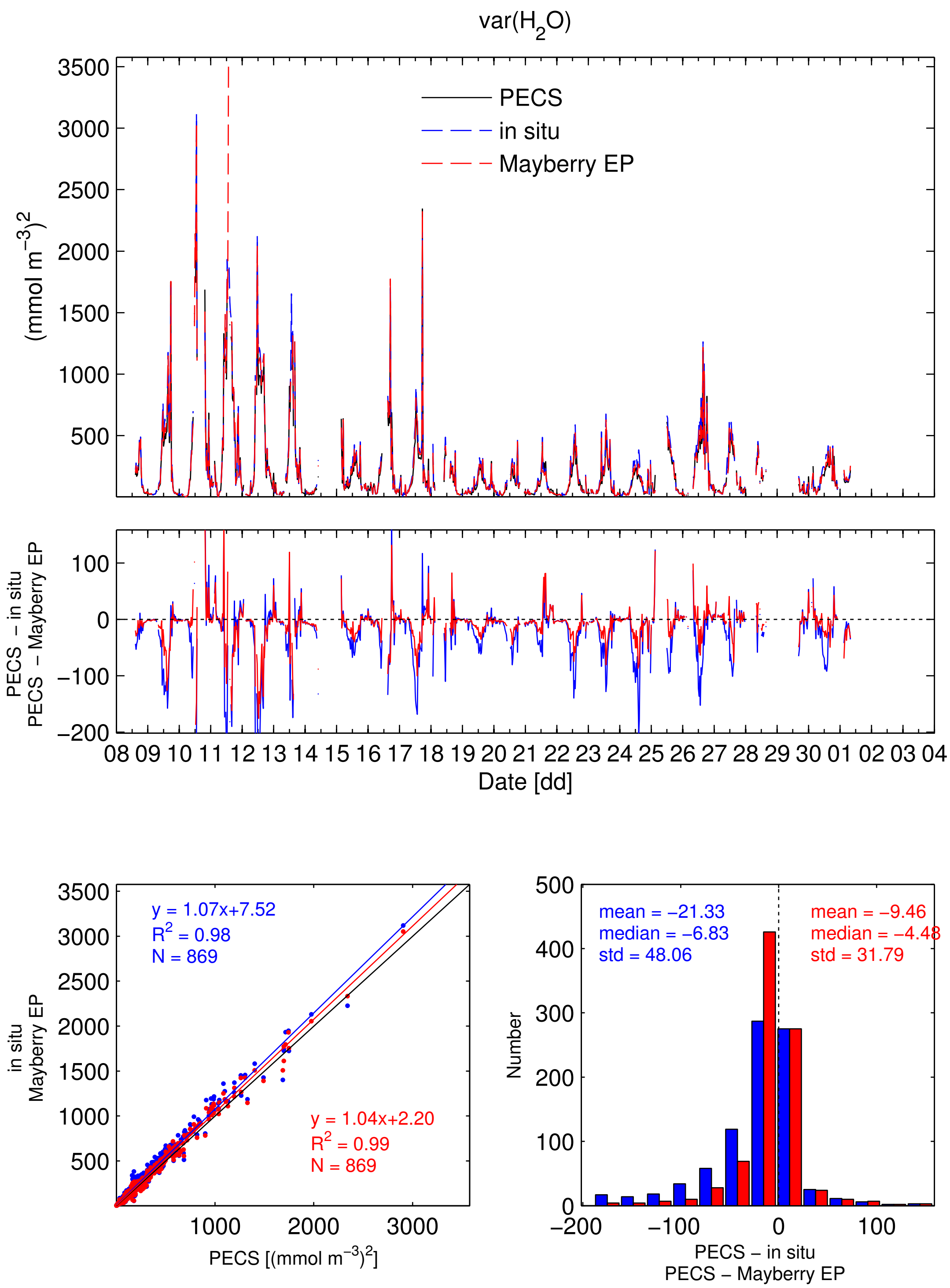

Figure 20 – Variance of water vapor mole density.

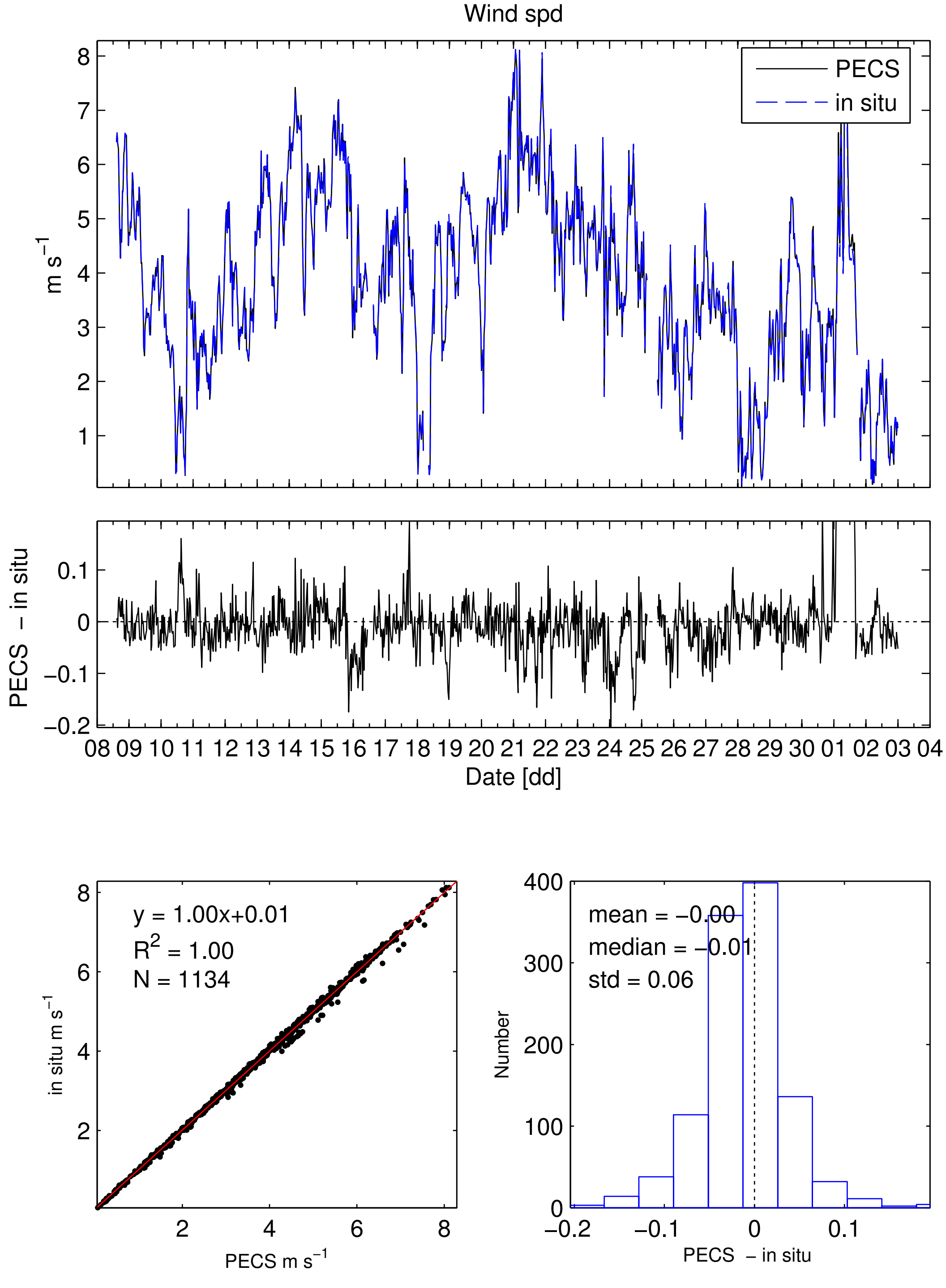

Figure 21 – Mean horizontal wind speed.

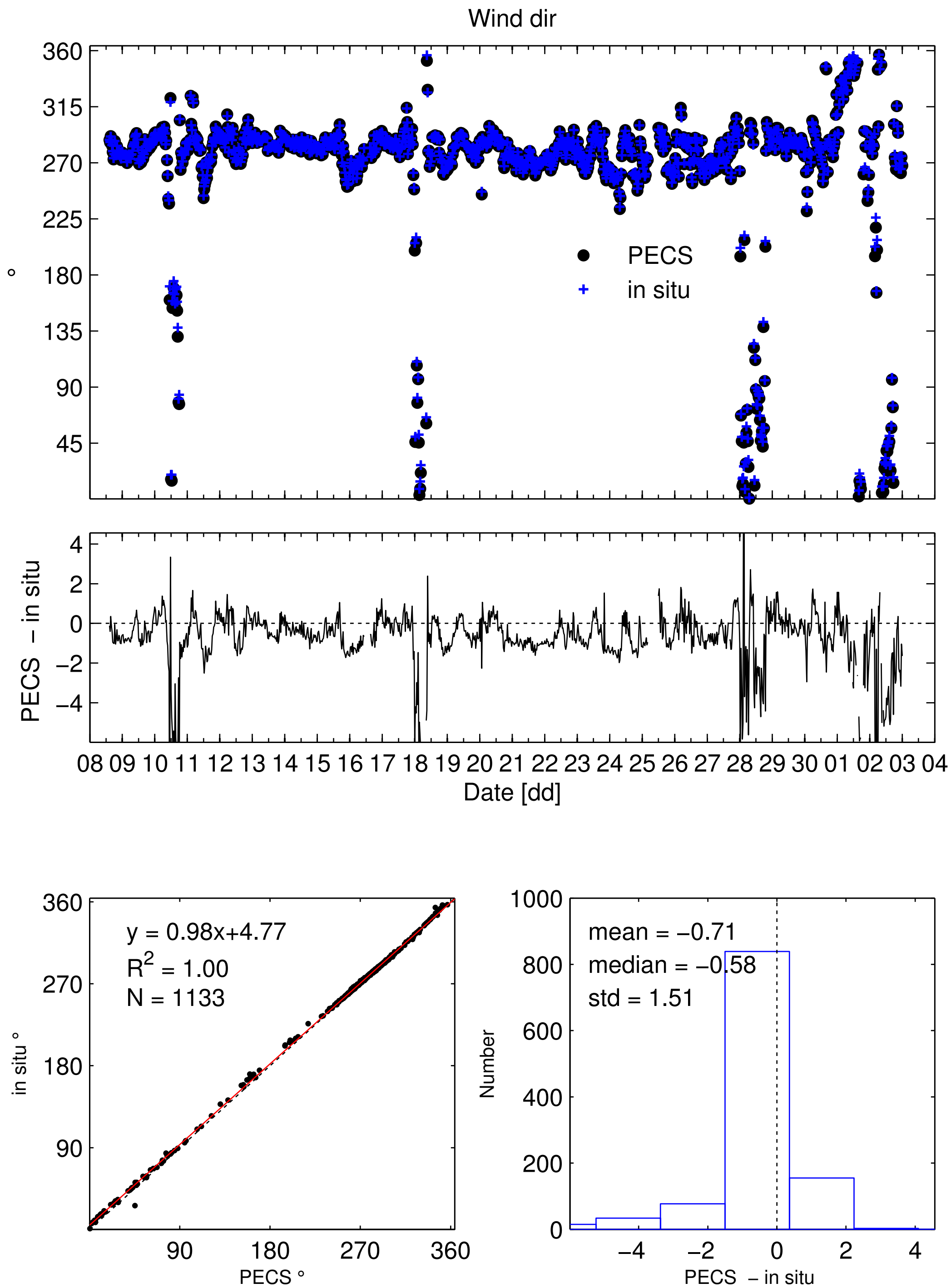

Figure 22 – Wind direction.

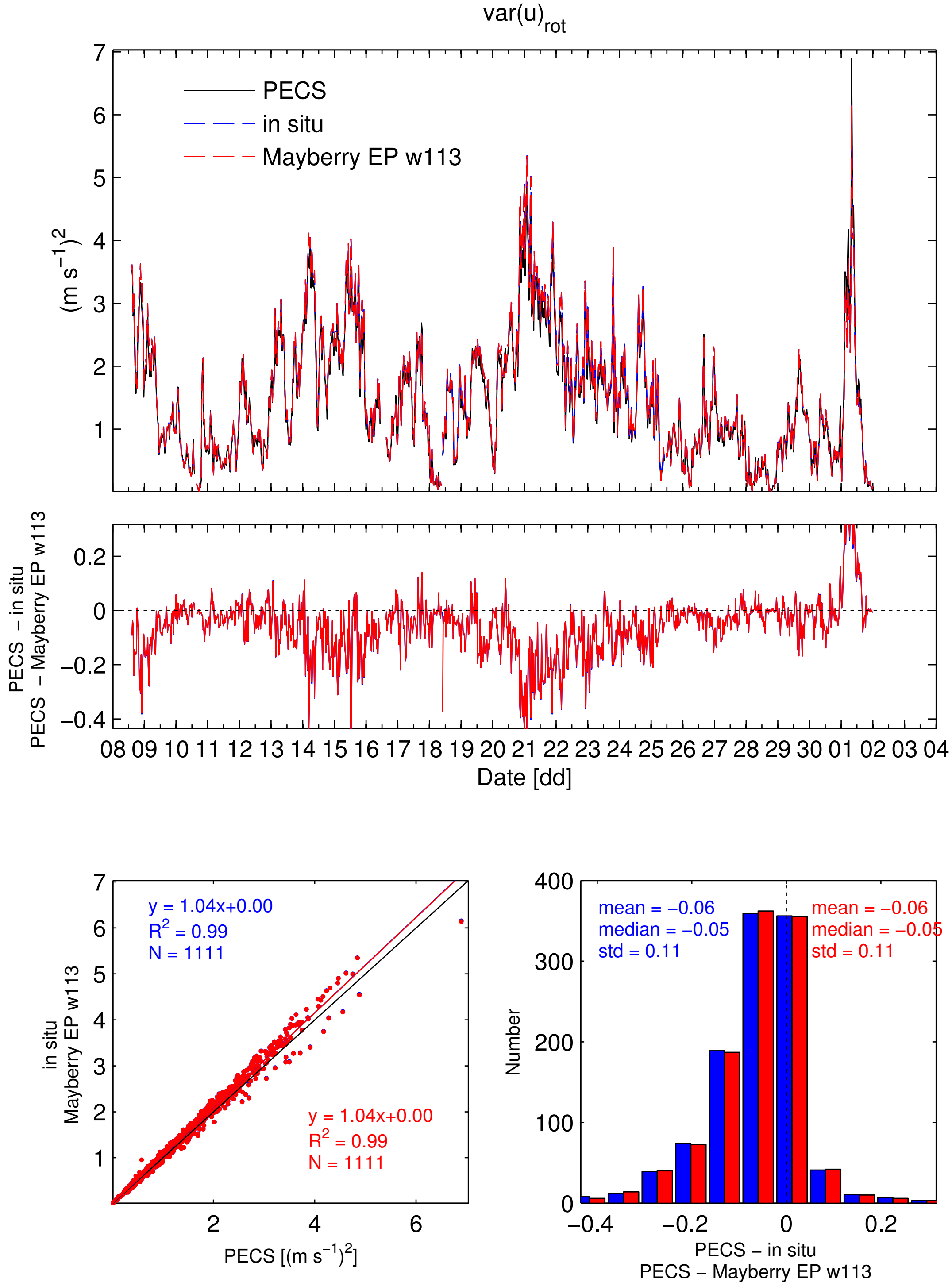

Figure 23 – Variance of along-wind component (u). Wind direction (WD) filter applied.

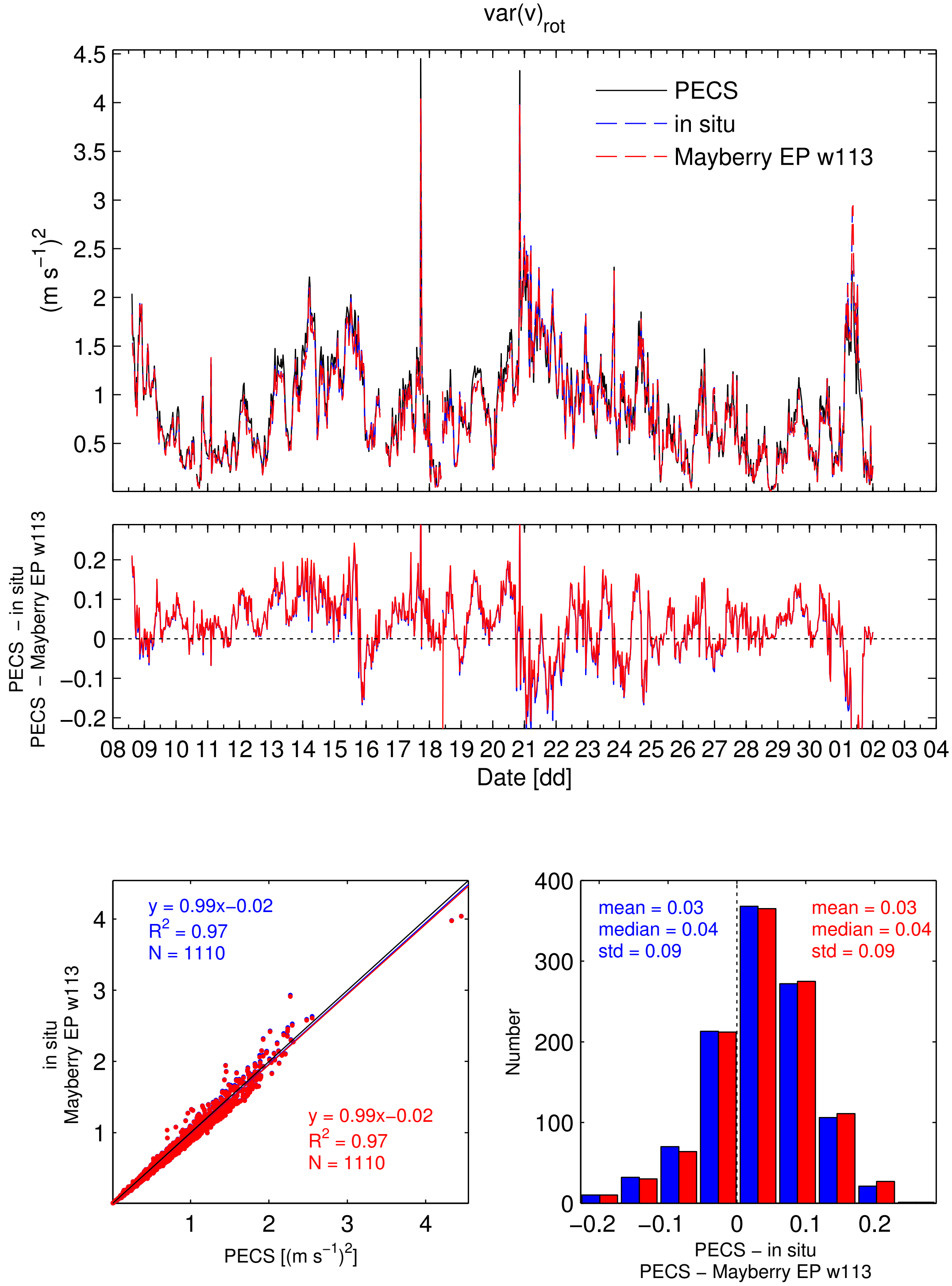

Figure 24 – Variance of cross-wind component (v). Wind direction (WD) filter applied.

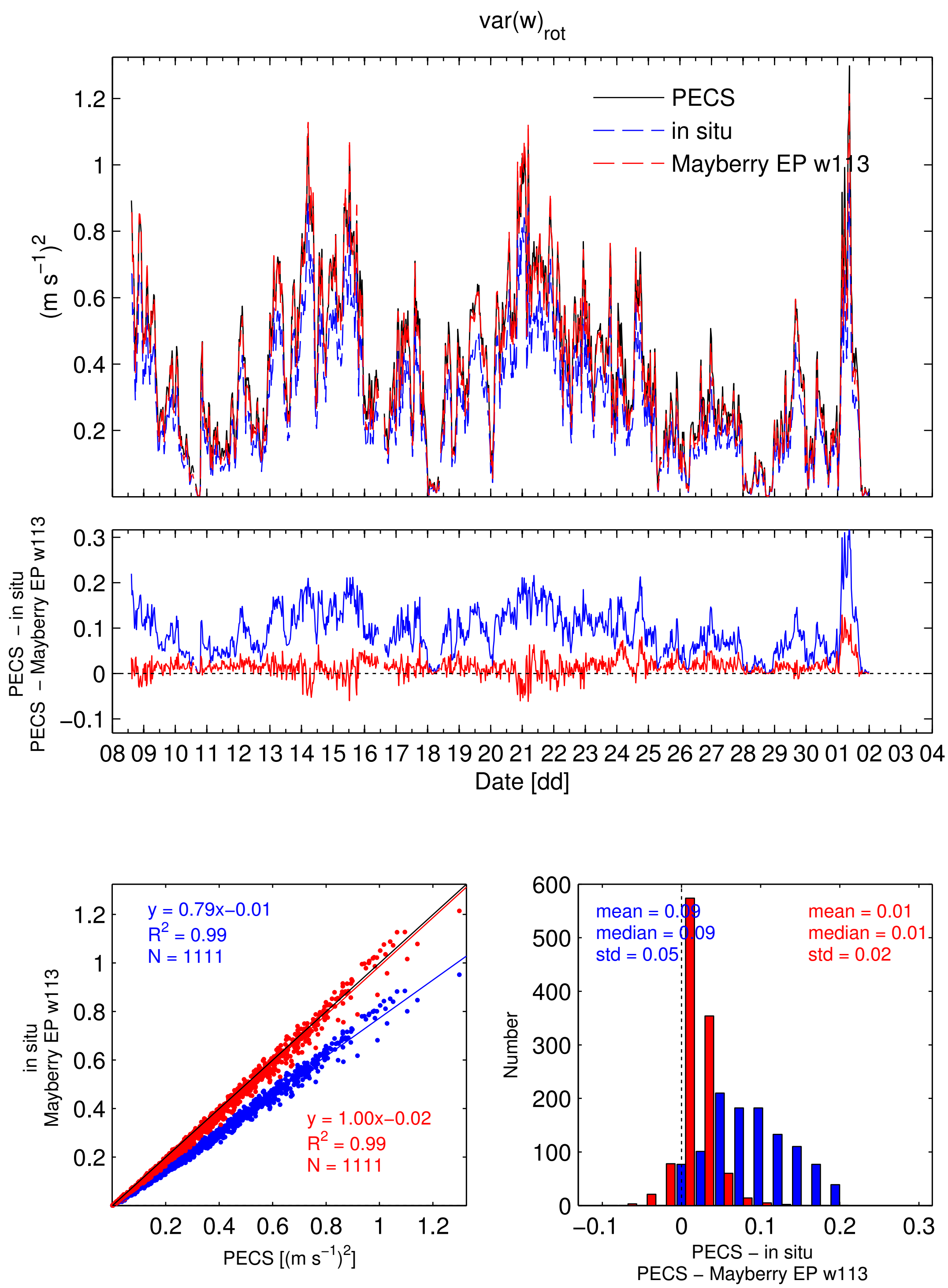

Figure 25 – Variance of vertical wind component (w). Wind direction (WD) filter applied.

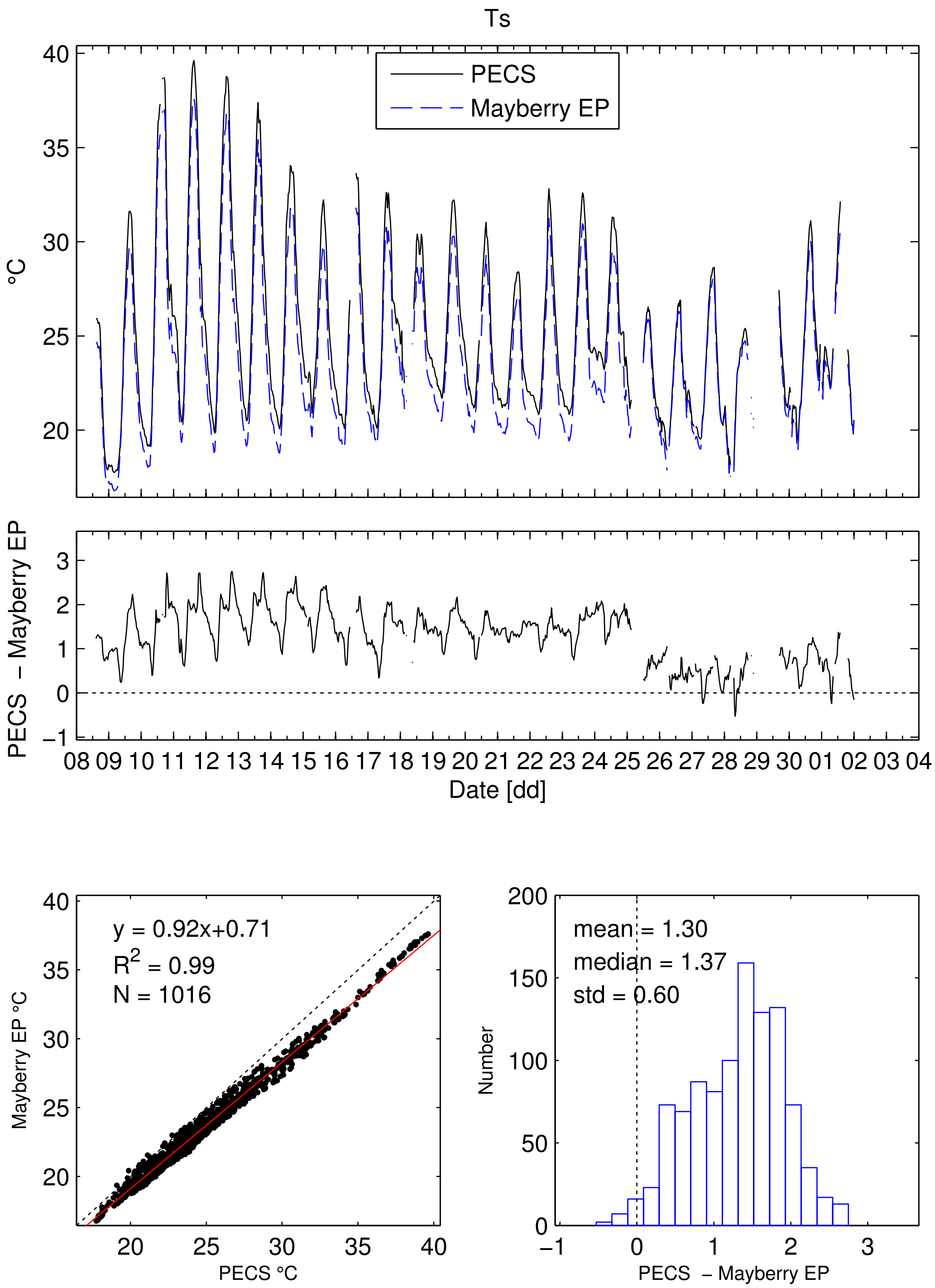

Figure 26 – Mean sonic temperature.

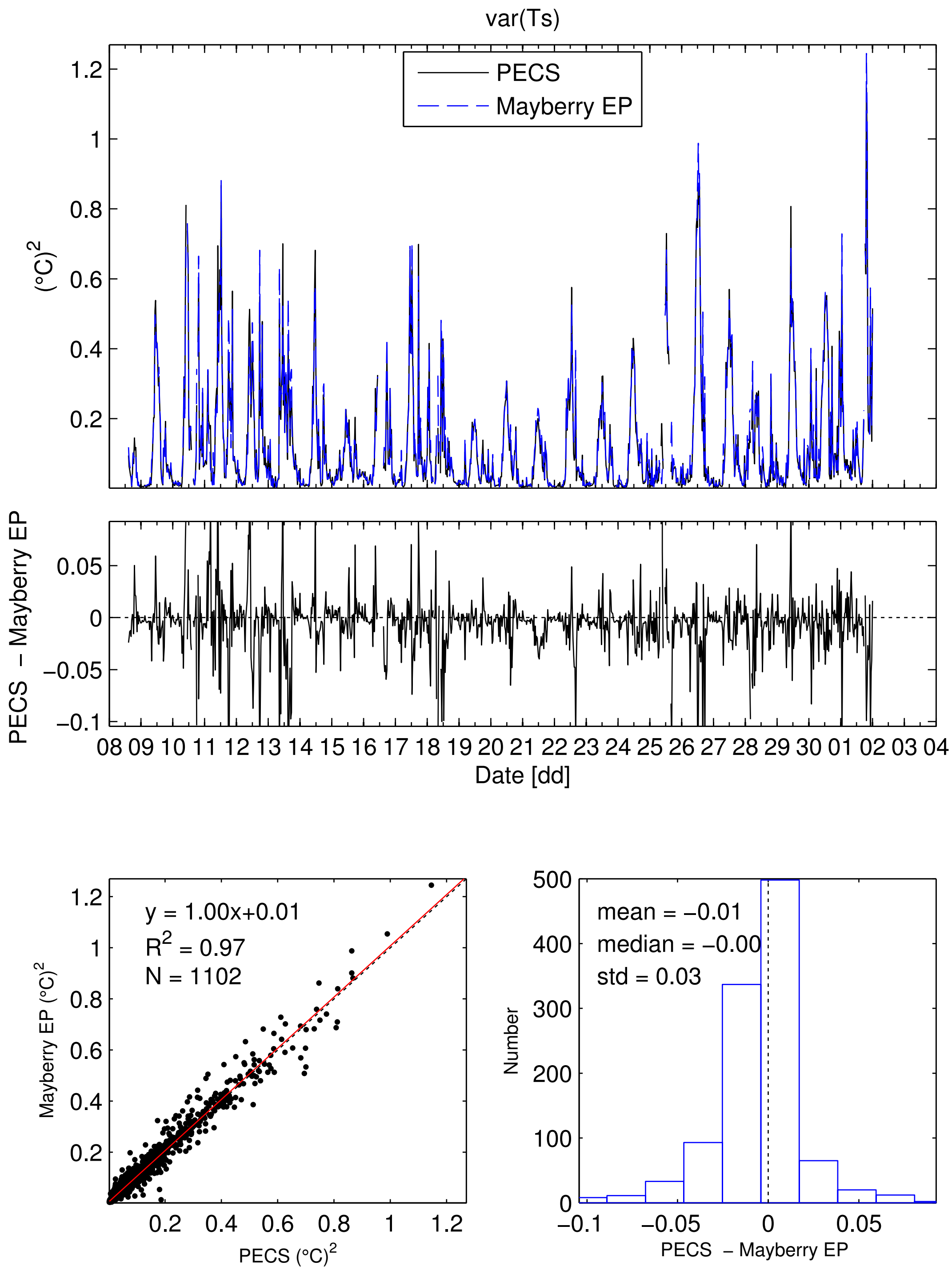

Figure 27 – Sonic temperature variance.

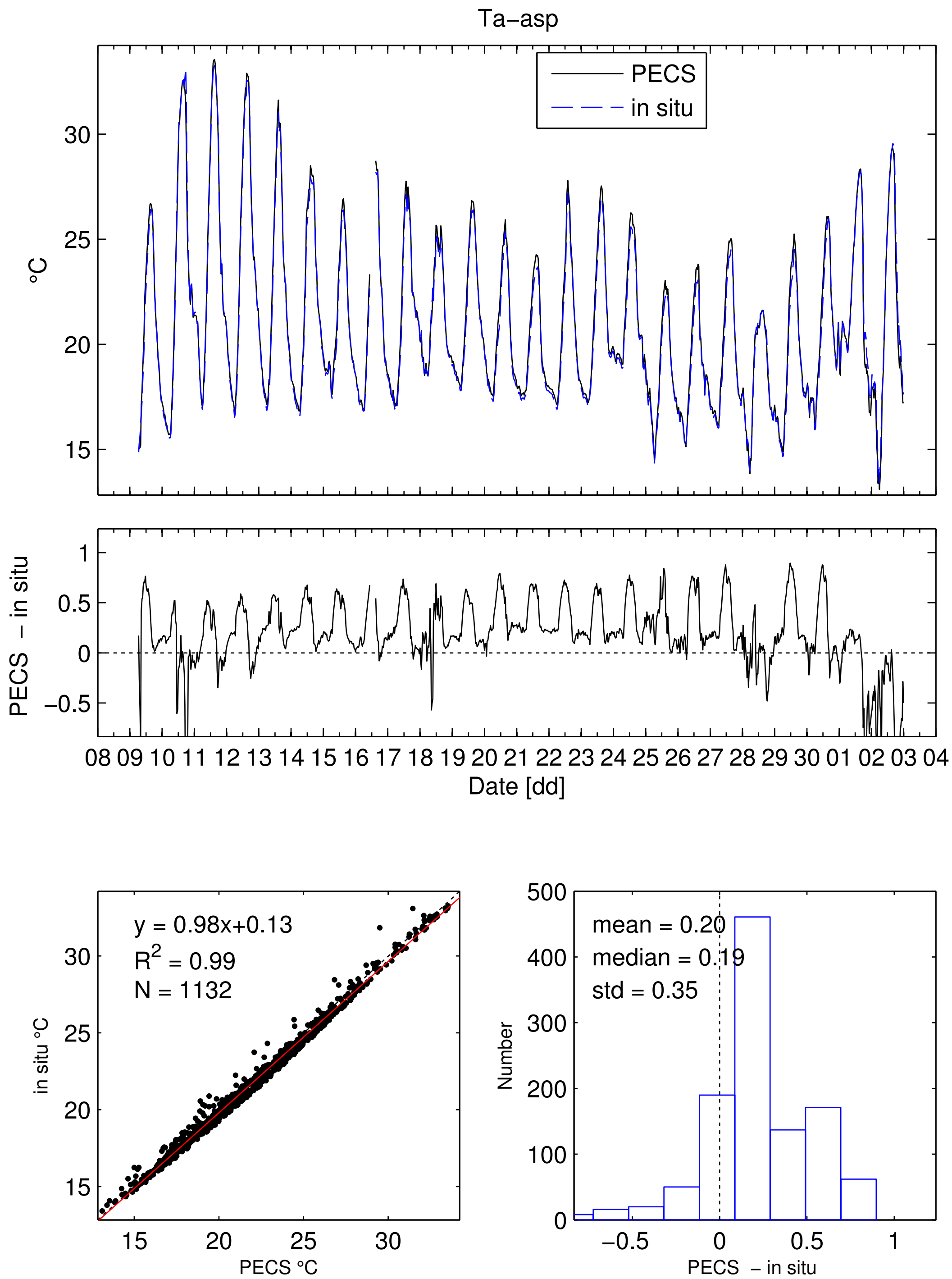

Figure 28 – Air temperature.

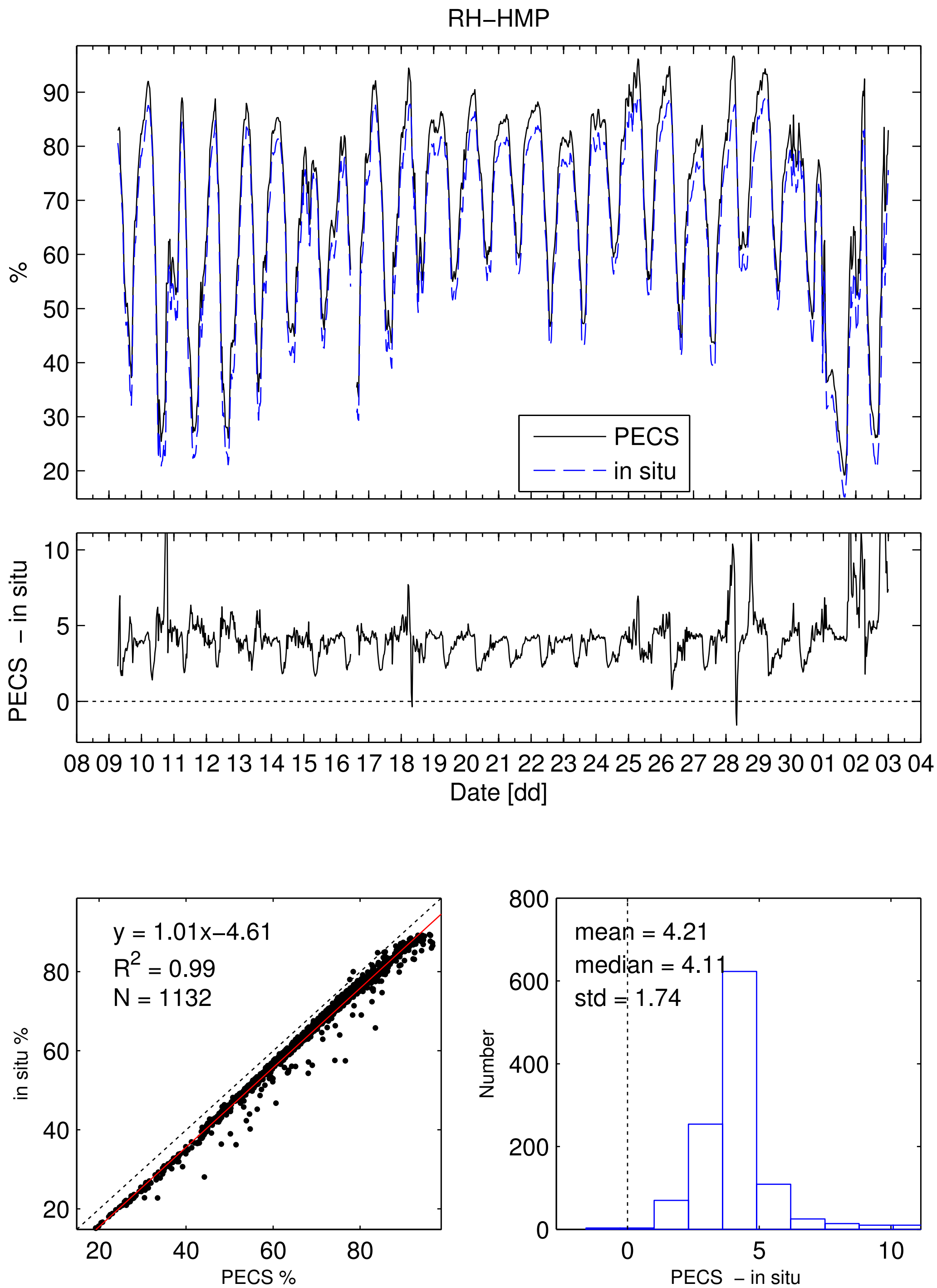

Figure 29 – Relative humidity.

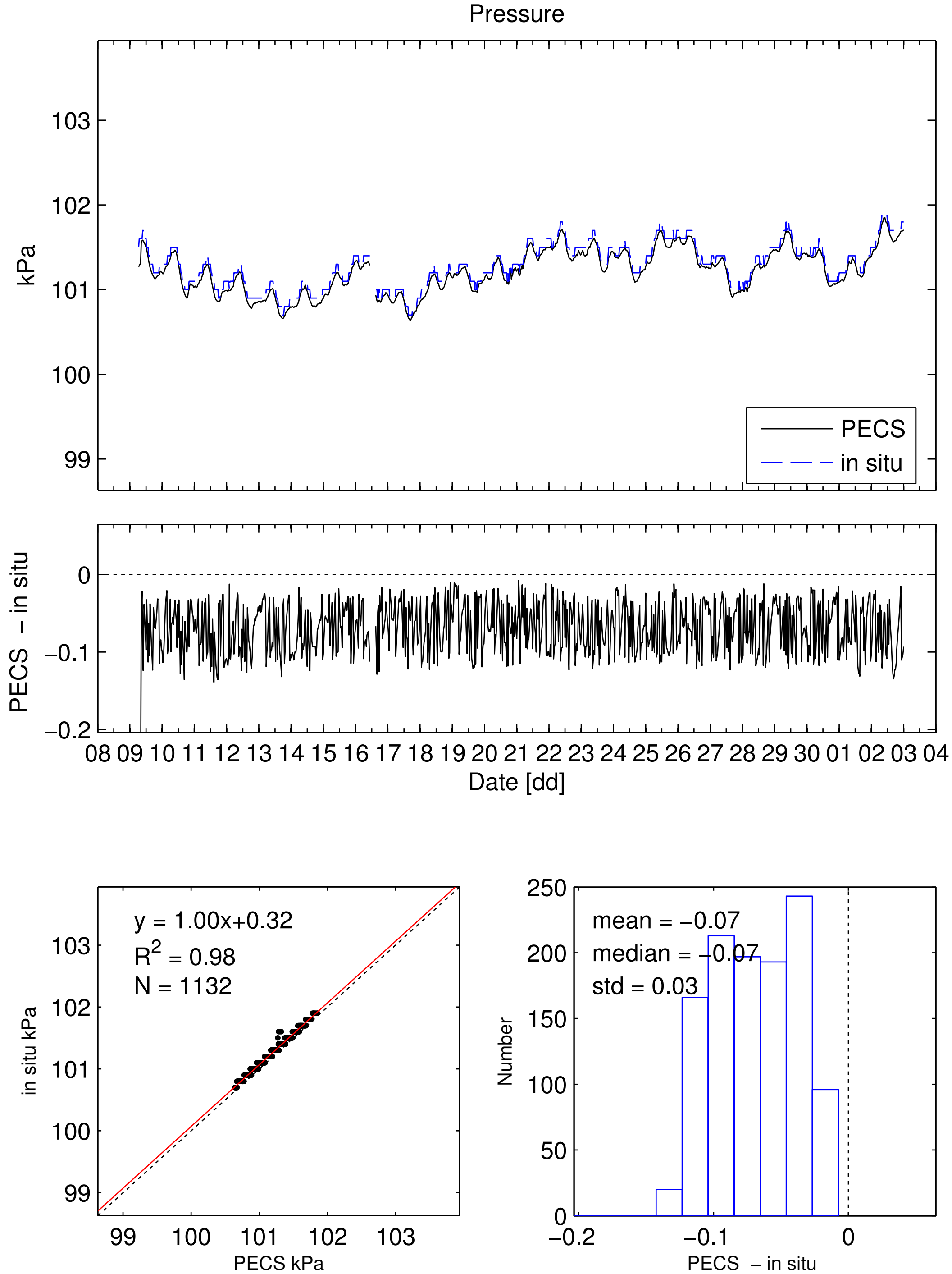

Figure 30 – Barometric pressure.

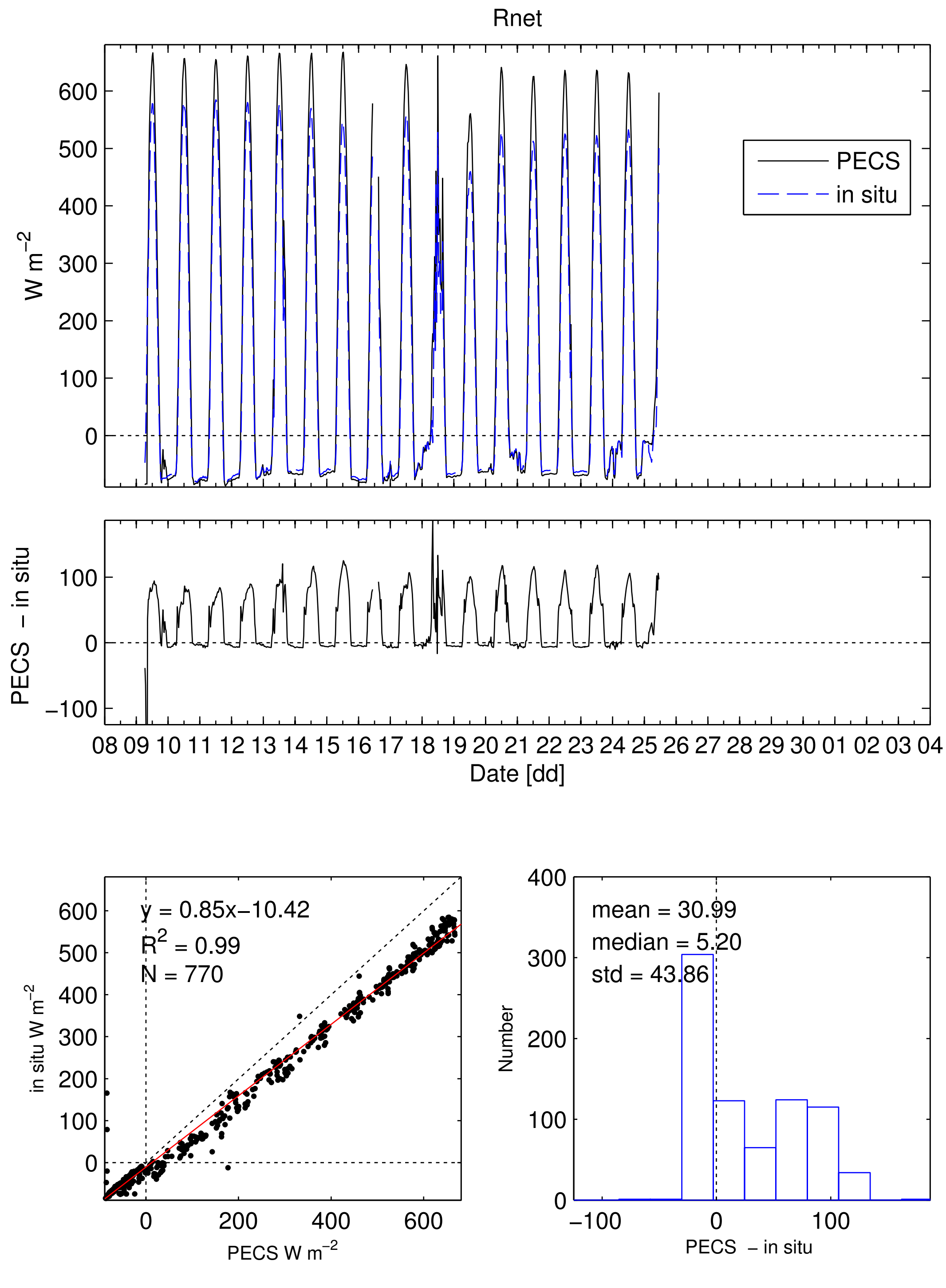

Figure 31 – Net radiation.

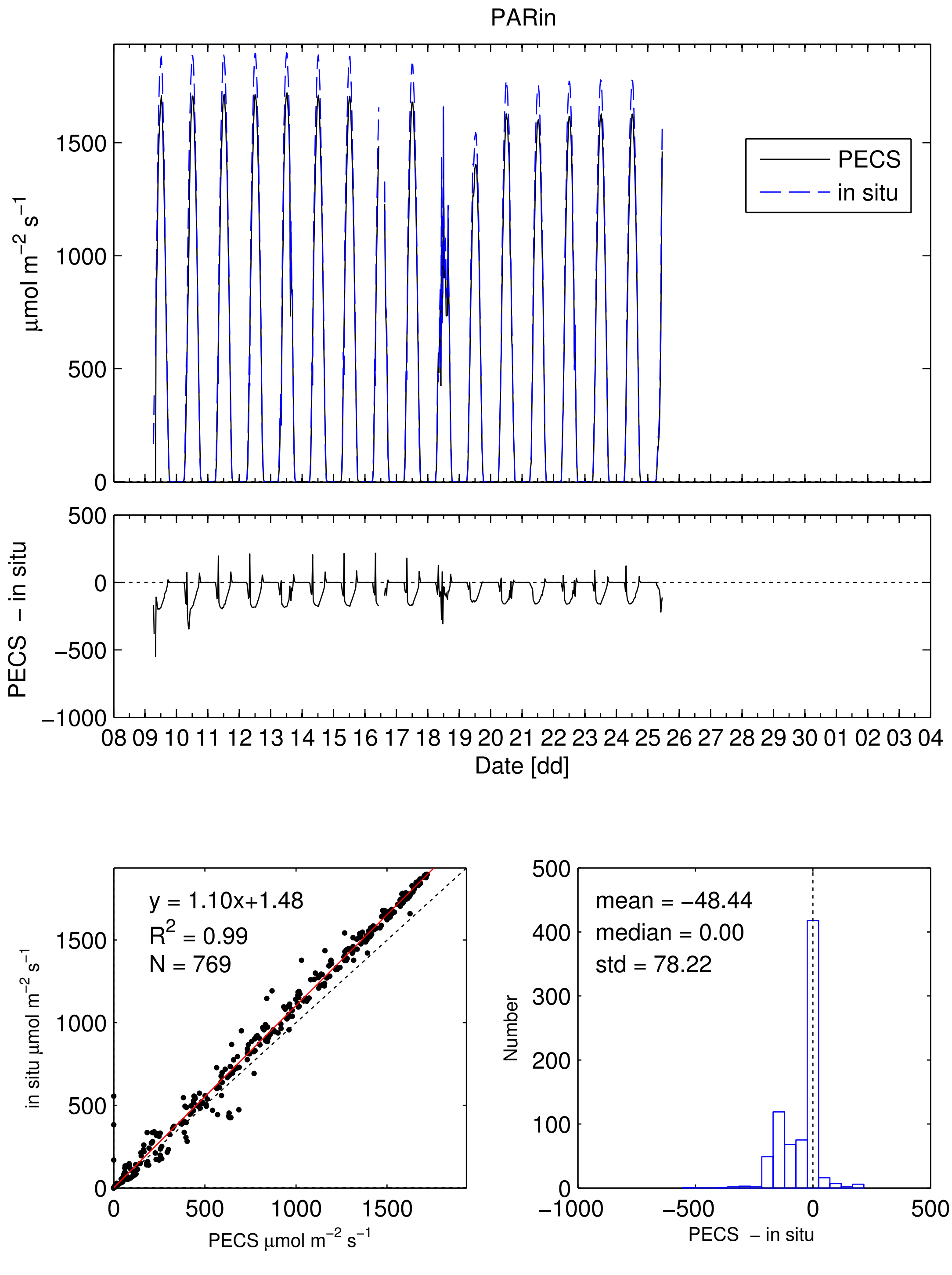

Figure 32 – Incoming photosynthetically active radiation (PAR).

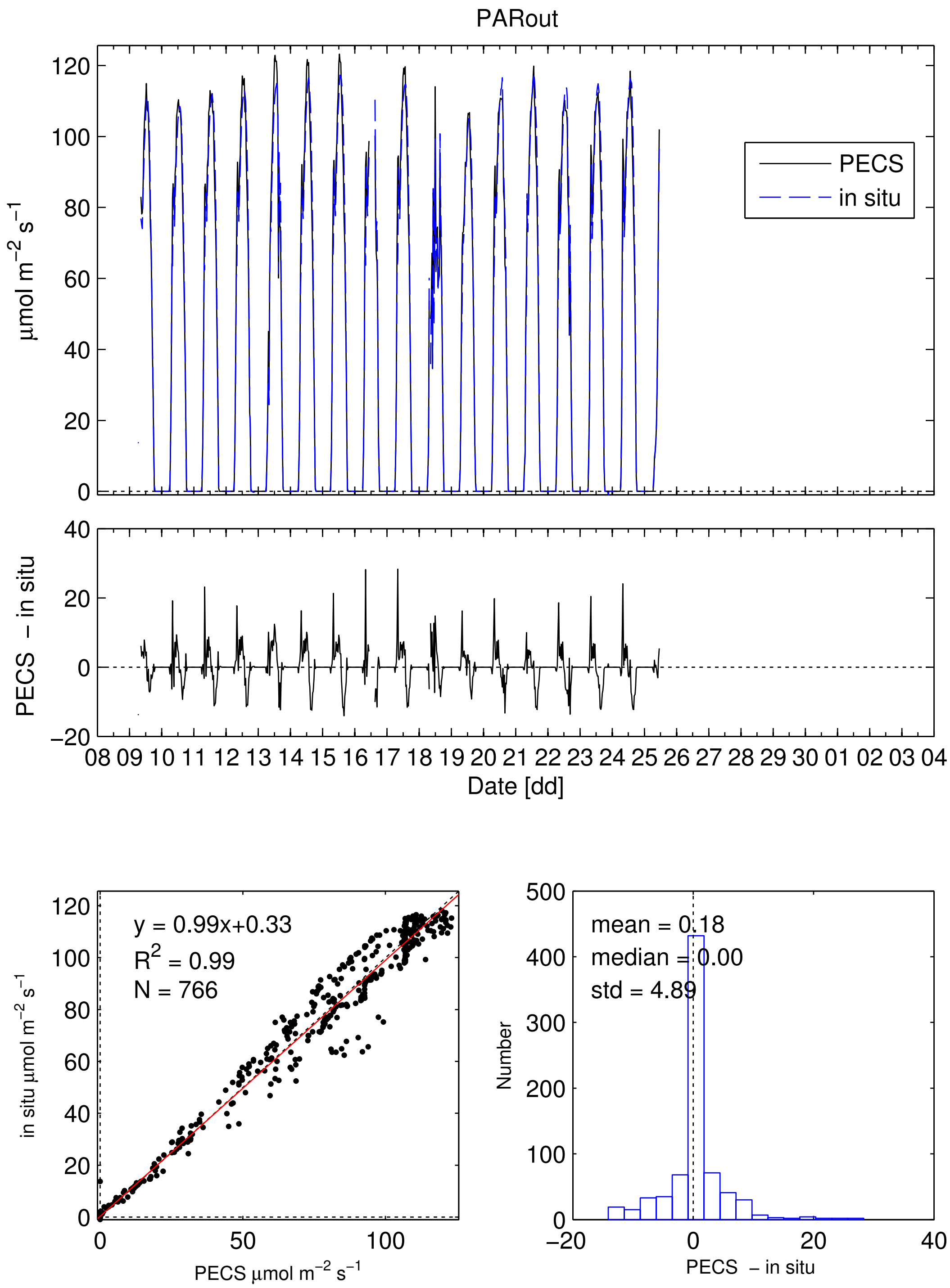

Figure 33 – Outgoing photosynthetically active radiation (PAR).

Site Name: Mayberry (US–Myb)
Visit Dates: 08 September – 02 October 2014

	Statistics				PECS				in situ			
	slope	ntercept	R2	N	mean1	std1	max1	min1	mean2	std2	max2	min2
CO2 flux	0.76	-0.27	0.93	884	-0.74	3.70	9.04	-12.37	-0.83	2.91	7.54	-9.43
Latent heat	0.89	0.84	0.97	911	92.15	66.15	370.13	-14.32	82.89	59.86	323.44	-6.87
Sensible heat	0.85	2.85	0.98	1053	11.89	70.05	258.93	-106.13	12.99	60.21	219.96	-83.91
u star	0.98	-0.01	0.98	1136	0.48	0.19	0.91	0.02	0.46	0.19	0.91	0.02
var(u)_{rot}	1.04	0.00	0.99	1164	1.42	0.97	6.89	0.01	1.47	1.01	6.15	0.01
var(v)_{rot}	0.99	-0.02	0.97	1163	0.84	0.50	4.45	0.01	0.81	0.51	4.04	0.01
var(w)_{rot}	0.78	-0.01	0.99	1164	0.36	0.24	1.30	0.00	0.27	0.19	0.95	0.00
CO_2	1.02	-0.37	0.91	889	16.41	0.36	18.00	15.44	16.37	0.38	17.82	15.43
H_2O	1.01	32.90	0.96	887	674.67	74.70	802.96	370.72	711.35	76.80	869.32	414.46
var(CO_2)	0.82	0.00	0.86	879	0.00	0.01	0.07	0.00	0.00	0.01	0.07	0.00
var(H_2O)	1.08	5.91	0.98	883	205.31	301.08	2905.37	2.83	227.01	327.67	3118.63	3.27
Ta-asp	0.98	0.13	0.99	1132	21.06	3.94	33.55	13.10	20.86	3.89	33.26	13.42
Ta-HMP	0.97	0.10	1.00	1132	21.46	4.02	34.22	13.47	20.86	3.89	33.26	13.42
RH-HMP	1.01	-4.61	0.99	1132	68.11	17.35	96.67	19.21	63.90	17.54	89.40	15.13
Pressure	1.00	0.32	0.98	1132	101.22	0.25	101.85	100.64	101.29	0.26	101.90	100.70
Wind spd	1.00	0.01	1.00	1134	3.89	1.65	8.11	0.07	3.89	1.65	8.12	0.05
Wind dir	0.98	4.77	1.00	1133	267.23	57.94	356.86	0.41	267.95	57.08	356.76	1.22
Rnet	0.85	-10.42	0.99	770	136.65	260.01	667.45	-87.65	105.66	221.76	584.51	-85.56
PARin	1.10	1.48	0.99	769	467.70	604.01	1720.10	0.00	516.14	666.49	1897.53	-0.95
PARout	0.99	0.33	0.99	766	37.72	44.65	123.19	0.00	37.55	44.32	118.05	-0.94

Table 1 – Summary of basic statistics from linear regression and for each system of compared variables.

Appendix 1 – Site information

General Site Information

Site name:	Mayberry
Mean canopy height (m); provide source of measurement:	(m)
Time zone of site data acquisition?	xST
Was PEC system sync'd to their local time? when?	Yes/No; date
Sampling frequency of fast response system:	? Hz

http://ameriflux.ornl.gov/fullsiteinfo.php?sid=227
Latitude (+N/-S): 38.0498 (38° 2' 59.2794")
Longitude (+E/-W): -121.7651 (-121° 45' 54.36")
Elevation: 0 m
Declination: 13.78° E (13° 46.8') on 2014-09-23

Site Instrumentation (make/model) - heights recorded below

Instrument	**Make/model**
Sonic anemometer	Gill Windmaster
Fast temperature sensor	N/A
IRGA#1 (open/closed)	LI-7500A
IRGA#2 (open/closed)	N/A
Other gas analyzer (describe)	LI-7700
Radiometer#1 (specify net or which component)	NRLite (down looking over water)
Radiometer#2 (specify net or which component)	NRLite (down looking over Tuli)
PAR#1	ParLite (down looking over water)
PAR#2	ParLite (down looking over Tuli)
PAR#3	ParLite (uplooking over Tuli)
Temp. sensor#1 (is aspirated?)	HPM45 (aspirated, build by Joe Verfaillie)
Humidity sensor (is aspirated?)	HMP45 (aspirated, build by Joe Verfaillie)
Barometer	
Wind sensor	
Vertical profile systems (temperature, winds, trace gases)	
Miscellaneous sensors (describe)	NDVI (down looking, build by Joe Verfaillie)
Miscellaneous sensors (describe)	NDVI (uplooking, build by Joe Verfaillie)
Miscellaneous sensors (describe)	infrared temperature sensor (over Tuli)
Miscellaneous sensors (describe)	infrared temperature sensor (over Tuli)
Miscellaneous sensors (describe)	water table height
Miscellaneous sensors (describe)	

Eddy covariance details (sensor heights, orientation, separation)

	PECS	**in-situ**
Sonic anemometer		

height [m]	4.88	4.88
orientation of sensor [o]	270	350
distance from tower/tripod [m]	0	0
orientation of boom (if different) [o]		
Open-path IRGA (measure relative to sonic)		
Vertical separation [cm] (pos if IRGA is above sonic)	-17.78	0
E/W separation [cm] (pos if IRGA is east of sonic)	+20.32	+35.56
N/S separation [cm] (pos if IRGA is north of sonic)	0	+12.7
Closed-path IRGA (measure relative to sonic)		
Vertical separation [cm] (pos if IRGA is above sonic)	-12.7	N/A
E/W separation [cm] (pos if IRGA is east of sonic)	+5.08	N/A
N/S separation [cm] (pos if IRGA is north of sonic)	+20.32	N/A
Inlet tube length [cm]		
Inlet tube inner diameter [mm]		
Inlet tube flow rate [lpm]		

Slow response details (sensor heights, orientation, separation

	PECS	**in-situ**
Radiometer#1 (over water) - height [m]	N/A	3.048
Radiometer#1 (over water)- orientation [o]	N/A	65
Radiometer#2 (over land) - height [m]	4.11	3.81
Radiometer#2 (over land) - orientation [o]	165	270
PAR#1(over water) - height [m]	N/A	3.048
PAR#1 (over water) - orientation [o]	N/A	65
PAR#2 & #3 (over land) - height [m]	4.11	3.81
PAR#2 & #3 (over land) - orientation [o]	165	270
Temp. sensor#1 - height [m] (HMP, asp)	3.35	4.88
Temp. sensor#2 - height [m]	3.35	N/A
Humidity sensor - height [m]	3.35	
Barometer - height [m]		
Wind sensor - height [m]		

Separation between systems (relative to in-situ)

System components	Vertical separation (specify units) (pos. if PECS above in-situ)	Horizontal separation (specify units)	Orientation to PECS (o)
Eddy covariance	0	48"	180
Radiometer#1	+52"	15 feet	45
Radiometer#2	+12"	90"	120
PAR# 3 (over land)	0	+20"	45

PAR# 1 (over water)			
Temp. sensor#1	-70"	90"	120

General Site Information- CH4

Site name:	Mayberry

Site Instrumentation (make/model) - heights recorded below

Instrument	**Make/model**
CH4 sensor (open/closed)	LI-7700
Miscellaneous sensors (describe)	

Methane details (sensor heights, orientation, separation)

	PECS	**in-situ**
Sonic anemometer		
height [m]	4.88	4.88
orientation of sensor [o]	270	350
distance from tower/tripod [m]	0	0
orientation of boom (if different) [o]		
Open-path CH4 (measure relative to sonic)		
Vertical separation [cm] (pos if IRGA is above sonic)	-12.7	-10.2
E/W separation [cm] (pos if IRGA is east of sonic)	+40.34	+25.4
N/S separation [cm] (pos if IRGA is north of sonic)	+17.78	-10.2
Closed-path CH4 (measure relative to sonic)		
Vertical separation [cm] (pos if IRGA is above sonic)		
E/W separation [cm] (pos if IRGA is east of sonic)		
N/S separation [cm] (pos if IRGA is north of sonic)		
Inlet tube length [cm]		
Inlet tube inner diameter [mm]		
Inlet tube flow rate [lpm]		

Appendix 2 – Photograph of site.

Photograph of eddy covariance sensors during the US-Myb site visit. The left mast held the PECS1 sensors. The right mast included the *in situ* eddy covariance sensors. The radiation and other sensors were deployed nearby.